Smith-Purcell free-electron laser

Levi Schächter
Department of Electrical Engineering, Technion–Israel Institute of Technology, Haifa 32000, Israel

Amiram Ron
Department of Physics, Technion–Israel Institute of Technology, Haifa 32000, Israel
(Received 13 February 1989)

We analyze the operation of a free-electron laser in an open periodic structure. When operated as an amplifier, it is shown that exponential gain can develop in such a device. An analytic expression for this gain is presented, and it is shown that this gain decays exponentially with the beam height above the grating; the gain dependence on the beam thickness is also analyzed. As the energy extraction rate is much higher in an exponential gain regime, we also investigate the operation of an oscillator based on the same concept. In this case, the Smith-Purcell radiation "provides the start-up" through a feedback system. The latter consists of several mirrors, which are placed in such a way that (1) only a wave with the desired frequency develops and, at the same time, (2) small deviations in the wave parameters due to the wave-beam interaction do not cause deflection of the wave from the feedback loop. The minimal current needed to sustain oscillations is given in an analytical form. Numerical calculations show that this current is more than three orders of magnitude lower than that necessary for an oscillator which operates in an algebraic gain regime.

I. INTRODUCTION

In 1953 Smith and Purcell[1] showed experimentally that electromagnetic (EM) radiation can be produced by an electron beam moving in an *open* periodic structure; this periodic structure was a metallic corrugated surface with spatial periodicity L and corrugation height a. The process was understood in terms of a simple model based on the oscillations of the image charges induced on the metallic surface, by the electrons. Later Toraldo di Francia[2] proposed the following way to explain the phenomena: the electromagnetic field produced by the moving electrons is described in the laboratory frame of reference as a superposition of evanescent waves. These waves are scattered by the grating. Since the periodic structure couples waves with different wave vectors, some of the scattered waves are propagating ones. In other words, part of the energy which initially was only reactive and was associated with the evanescent waves is now "transformed" into radiation power, by the grating.

Based on the Smith-Purcell (SP) effect, it was suggested to construct a laser that amplifies electromagnetic waves in frequency and power domains that are not achievable with the present technologies. This device is a member of a large group—the so-called free-electron laser (FEL's)—which benefit from the interaction of energetic electron beams with EM waves in periodic structure. Yariv and Shih[3] have calculated the total power transferred by an electron beam to a TM electromagnetic wave when moving in a *closed* slow wave structure, i.e., in a waveguide with corrugated walls. They assumed that the EM field amplitude is practically unaffected by the motion of the charged particles. Each particle induces an EM field and the net transferred radiation power is due to a constructive-interference effect of all these contributions. For a thin and dilute beam, the authors have shown that the power transferred in a finite-length device has similar characteristics to the case in which an electron beam interacts with a TEM wave in a periodic magnetic field. Later Gover and Livni[4] have generalized the analysis to include variations of the EM amplitude due to the energy exchange with the beam; it was shown that this process can cause an *exponential* growth in the field amplitude. They also compared this regime with the one described in Ref. 3, i.e., *nonexponential* gain, and they suggested that the latter occurs when the slip between the particles' average velocity (V_{av}) and the synchronous wave phase velocity (V_{ph}) is larger than the electrons' thermal velocity (V_{th}), i.e., $|V_{ph}-V_{av}| \gg V_{th}$; the exponential gain regime occurs when the deviation from synchronization is small, i.e., $|V_{ph}-V_{av}| < V_{th}$. In their analysis the space-charge effects were neglected, or in other words, the divergence of the electric field in the beam domain was neglected. The last two works[3,4] treat the SP device as a *closed* slow wave structure, and calculate the energy exchange as in the traveling-wave amplifier (TWA).

The first attempt to calculate the total power exchange between an EM wave and an electron beam moving above an *open* corrugated surface was reported by Wachtel.[5] According to his approach an electromagnetic wave which impinges on a corrugated surface is scattered into a variety of waves; one of these is almost synchronous with an electron beam which moves parallel to the grating. The amplitude of this synchronous wave is uniform, and so it is considered to be kept, even when the beam is injected. As in the case of Ref. 3, the electrons oscillate due to the presence of the field, and therefore they induce an additional EM field. The net power converted to radiation is due to a constructive interference effect. The functional form of Wachtel's expression for the power ex-

change is quite similar to that reported in Refs. 3 and 4; however, there are two major differences between these two results. (a) The wave vector within a waveguide is totally determined by the wall's dimensions and the frequency (but not by the incident wave vector) whereas in an *open* grating, the scattered wave vector is determined by the *incident wave vector* and the system periodicity. (b) The second difference is due to the fact that the entire interaction domain is illuminated—in contrast to TWA where only the device entrance is illuminated. In the present study some of the "constraints" in Wachtel's analysis are released, namely, the electron beam is not assumed to be very thin, it is also assumed to be at a finite height above the grating and finally, the coupling between the interaction harmonic and the radiating ones is not introduced as a parameter of the problem.

Although it is expected that in the exponential gain regime more energy can be extracted from the beam, all previous studies of open periodic structures investigated only the nonexponential gain regime. Leavitt *et al.*,[6] for example, have carried out experiments and calculations for the orotron in the millimeter wave region. In their analysis, the authors have considered a more complex cavity which consists of a corrugated surface and above it, a large concave mirror. As in the other cases, the induced current is calculated assuming that the amplitude of the EM wave is maintained constant along the grating and thus the power transferred to radiation is a result of a constructive interference effect. In this case the calculations are similar to Refs. 3 and 5, and only the field distribution makes them more complicated. Nonexponential gain was recently investigated by Bratman *et al.*[7] in *close* periodic structures, however, since the beam was injected very close to the grating, the system effectively acts as an open device.

In the present paper we investigate a Smith-Purcell amplifier (SPA) and a Smith-Purcell oscillator (SPO) in their *exponential* gain regime.[8] Let us now briefly describe the SPA operation. A SPA is composed of a corrugated surface and a beam of electrons whose average velocity parallel to this surface is V_0. When operated as an amplifier, this device is illuminated by an electromagnetic plane wave which is scattered by the grating into a wide *spatial* spectrum of propagating and evanescent waves. The phase velocity of the evanescent waves is smaller than c, the phase velocity of a plane wave in vacuum; therefore the beam can exchange energy with one (or more) of these waves. Assuming that the beam is *cold,* there is only a single evanescent wave which effectively exchanges energy with it—this will be called the synchronous wave (SW). As a consequence of this process the amplitude of the SW is changed; this change is transmitted by the grating to all other waves. In particular, we are interested in the change which occurs in the propagating waves, since these can be measured far away from the grating. The linear relation between the "input" waves and the "output" ones is called the response function of the amplifier. This function is determined in terms of the EM properties of the grating, the beam characteristics, and the frequency. When poles appear in the analytical continuation of the response function, one of them may be responsible for the exponential increase of the amplitude of the field along the interaction domain. These poles occur due to the grating support of a synchronous wave.

On the basis of the analysis of the amplifier mode of operation, we continue and study a Smith-Purcell oscillator. This device consists of a grating and a beam identical to those of the SPA, as well as a feedback system (mirrors) which returns back to the grating part of the scattered waves. In a SPO only the electron beam is injected into the system, and the radiation is created by the beam. It is this radiation that provides the startup to our oscillator. A part of this EM flux is returned back by the feedback, to the grating domain, where the beam now plays an additional role (to that of a source) as an active medium. As we have just discussed in the context of SPA, we can imagine a situation in which this incident wave is amplified by the active component (grating plus beam) to such an extent that it "overcomes" the inherent losses in the system, e.g., scattering process and the materials' finite conductivity—then oscillations can be sustained. Using the response function of the amplifier, the condition for such oscillations to be maintained is determined. The minimal (threshold) current necessary for these oscillations to develop is then calculated approximately assuming that the grating supports the SW. This current is compared with that of Wachtel's scheme and it is found to be much lower.

The electron dynamics is calculated within the fluid description. As the intensity of the EM field involved in the process is relatively low, the equations of motion can be linearized. Also the transients in space and in time are neglected. In many experiments a dc magnetic field is applied in order to avoid the beam divergence. If this field is large enough, we can consider the motion as one dimensional.

In the magnetic bremsstrahlung FEL the particles move in a periodic magnetostatic field and in a radiation field. In Smith-Purcell FEL there is no static field, but instead the EM field is subject to periodical boundary conditions. It is proposed here to formulate the boundary problem in terms of a reflection matrix—which couples the amplitudes of the outgoing and incoming waves (both propagating and evanescent). This formulation is convenient in a periodic structure, since the component of the wave vector parallel to the grating can be "decomposed" into $k_n = k + (2\pi/L)n$ where n is an integer and k is the wave-vector projection in the first Brillouin zone ($|k| < \pi/L$), and k is a conserved quantity in the scattering process. In other words, the periodic structure, or in our formulation—the reflection matrix—couples between waves of all different n's. It should be emphasized that formulation of the scattering process in terms of the reflection matrix does not solve the boundary condition problem; it only provides a convenient scheme to investigate the physical processes in the presence of the grating. This approach is correct only for very long devices, say, at least 100 periods. We do not consider in the present study margin effects. The reflection matrix in the context of periodic structures is not a new concept; its properties were investigated by Uretsky[9] in 1965. Peng *et al.* and

Waterman[10] have also determined the reflected waves from a periodic dielectric layer utilizing the reflection matrix. In this present work we do not attempt to investigate the boundary problem (except two cases where we demonstrate our results with numerical examples), and therefore only a short discussion of some of the methods involved is brought in the next paragraph.

Scattering of EM waves from gratings has been thoroughly investigated (see Petit[11]). It started about 80 years ago when Rayleigh[12] published his pioneering work on wave scattering from a sinusoidal grating. In his work he described the reflected wave above the grating top as a superposition of Floquet waves which either decay exponentially, in the case of the evanescent waves, or propagate from the grating outward. Between the grooves the field has to be described as a superposition of up and down going (propagating) waves or decaying and growing (evanescent) waves. At the limit of low corrugation depth, a, relative to the EM wavelength λ, he asserts that the down going and the growing waves in between the grooves are negligible. What remains are outgoing (and decaying) waves, which are assumed to be identical with the ones scattered above the grooves' top—this is the Rayleigh hypothesis. Such a superposition of Floquet waves together with the incident wave satisfy the boundary conditions on the grating surface. The reflected waves are expressed as powers of this small parameter a/λ. The Rayleigh hypothesis was a subject of controversy[13] for many years. Although this hypothesis was extensively used in the literature (see Ref. 11, Chap. 1), its applicability to the Smith-Purcell effect is questionable since a/λ is not necessarily small. Other calculations of the scattering process based on the Wiener-Hopf method were successfully performed.[14,15] This method is not limited to the low-frequency domain; however, it is applicable only to a few geometries. An equivalent analytical method was employed by DeSanto[16,17] for calculating the waves reflected by a grating of a simple geometry. In general, in order to evaluate the reflection matrix of a grating with an arbitrary geometry, it is necessary to resort either to integral or differential methods (Ref. 11, Chaps. 1, 3, and 4). These in turn necessitate a considerable amount of numerical work. For very few geometries (such as rectangular or triangular grooves) the field in the grooves can be described by using normal-mode expansion and the evaluation of the reflection matrix is relatively simple (see again Ref. 11, Chap. 1).

The outline of this paper is as follows. In Sec. II we start with the description of the active component. After a short general introduction, we discuss in detail the formulation of the boundary problem of the periodic structure in terms of the reflection matrix. We explicitly demonstrate its calculation for a relatively simple geometry. The use of the reflection matrix is then demonstrated for the Smith-Purcell effect. This will provide us a better physical insight to the operation of SP FEL as an oscillator. We conclude this section with a discussion of the electron dynamics.

Section III is dedicated to the study of the response of the Smith-Purcell amplifier to an external EM wave. The solution of the EM field problem is presented in Sec. III A and the response function is determined. Since it turns out that the poles of this function depend only on a single diagonal term of the reflection matrix, we can analyze their behavior using a simple model of a dielectric slab placed above a high-conductivity material. This analysis is performed in Sec. III B assuming that the grating supports electromagnetically the propagation of a synchronous wave. In this section we show that an exponential gain may occur in a SPA. The dependence of the gain on the beam parameters is also discussed here.

The analysis of the Smith-Purcell oscillator is opened with a general discussion (Sec. IV A). The design principles of the feedback system are thoroughly investigated in Sec. IV B. After we establish the feedback properties, we determine the condition for self-sustained oscillations in Sec. IV C. The threshold current which is the minimal injected current necessary for these oscillations to exist is calculated in Sec. IV D much in the spirit of gain evaluation in Sec. III B. In Sec. V we finally summarize the results of this study.

II. THE ACTIVE COMPONENT

A. General description

We consider a metallic grating, with its surface in the x-y plane. This surface has a periodicity L in the x direction and the y axis is parallel to the grooves which are uniform in this direction. The particular geometry of each unit cell is not important for the present purposes. The top of the grating is taken to be the $z=0$ plane. The grating is assumed to be very long compared to its spatial periodicity, say at least 100 periods, so that spatial transients, which decay after about 3–5 periods, have a negligible effect. A monochromatic electromagnetic plane wave—oscillating with an angular frequency ω—is incident upon the diffraction grating in the x-z plane with an angle θ with respect to the z axis (see Fig. 1). This wave is described by the y component of the magnetic field

$$H_y^{(\mathrm{inc})}(x,z,\omega)=H_0\exp\left[-j\frac{\omega}{c}\sin\theta x+j\frac{\omega}{c}\cos\theta z\right];$$

the time dependence is $e^{j\omega t}$. An electron beam is injected into the system. The electrons' average velocity is $\mathbf{V}_0=V_0\mathbf{1}_x$ and the beam density is n_0. The total EM field in the beam excites a current density $\mathbf{J}(x,z,t)$ which we assume has only a single component J_x. This would happen in a guiding dc magnetic field. The total EM field is composed of the primary and secondary field, which is a solution of the nonhomogeneous wave equation

$$\left[\nabla^2+\frac{\omega^2}{c^2}\right]H_y^{(\mathrm{sec})}(x,z,\omega)=-\frac{\partial}{\partial z}J_x(x,z\omega)\,. \tag{2.1}$$

Our purpose in this section is to determine and analyze this secondary field, subject to (a) the boundary conditions on the field and (b) the current density as determined by the equations of motion of the electrons. These two are discussed in Secs. II B and II C.

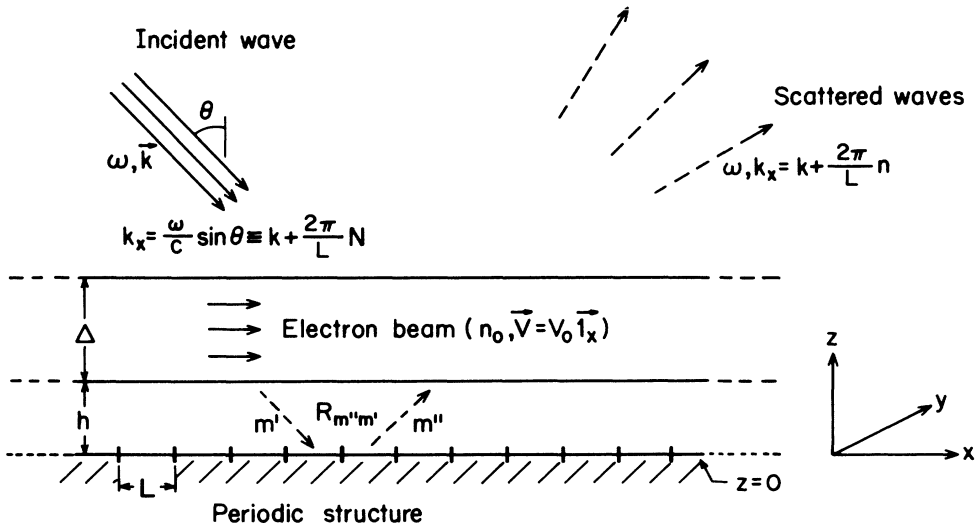

FIG. 1. The basic configuration of the Smith-Purcell amplifier (SPA). A beam of electrons is moving above a metallic grating. This system is illuminated by an incident wave whose field is oscillating with an angular frequency ω; θ is the angle between the wave vector and z axis. The reflection process at the grating top is described in terms of the reflection matrix R_{nm}. The electrons' average velocity is V_0 and their average density is n_0; the beam thickness is Δ and its width is Δ_y. Between the beam and the grating there is a gap of a height h. L is the grating periodicity.

B. Reflection matrix

1. General formulation

In this subsection we leave out the beam and concentrate on the boundary condition problem; we demonstrate that it is possible to represent the boundary conditions, imposed by the grating, in terms of a reflection matrix. This formulation is based on the Floquet decomposition of the wave vector along the x direction. We write the wave vector in the x direction, k_x, as

$$k_x = k_n = k + (2\pi/L)n \ , \tag{2.2}$$

where n, the harmonic label, is an integer, $2\pi/L$ is the grating wave vector, and k is defined in the first Brillouin zone ($|k| < \pi/L$). The advantage of this notation is that in a scattering process k is conserved, and the periodic structure couples between all the harmonics. An incident wave, which oscillates with a frequency ω, is given by

$$H_y^{(\mathrm{inc})}(x,z,\omega) = H_0 \int_{-\pi/L}^{\pi/L} dk \sum_{n=-\infty}^{\infty} F_n(\omega,k) e^{-jk_n x} e^{\beta_n z} \ , \tag{2.3}$$

where $\beta_n = [k_n^2 - (\omega/c)^2]^{1/2}$. Obviously for the incident plane wave, which was previously introduced, the spatial spectrum, i.e., the wave amplitude, reads

$$F_n(\omega,k) = \delta_{nN}\delta(k - k_0) \ . \tag{2.4}$$

Here δ_{nN} and $\delta(k-k_0)$ are the Kronecker and Dirac δ functions, respectively, while the parameters N and k_0 are determined by Eq. (2.2) substituting $k_x = (\omega/c)\sin\theta$, i.e.,

$$\frac{\omega}{c}\sin\theta = k_0 + \frac{2\pi}{L}N \ . \tag{2.5}$$

The general expression for the scattered field is similar to Eq. (2.3), except that radiation with β_n imaginary propagates away from the grating, and for real β_n the field decays exponentially, that is,

$$H_y^{(sc)}(x,z,\omega) = H_0 \int_{-\pi/L}^{\pi/L} dk \sum_{m=-\infty}^{\infty} D_m(\omega,k) e^{-jk_m x} e^{-\beta_m z} \ . \tag{2.6}$$

The most general relation between the amplitudes $D_m(\omega,k)$ and $F_n(\omega,k)$ is

$$D_m(\omega,k) = \sum_{n=-\infty}^{\infty} R_{mn}(\omega,k) F_n(\omega,k) \ , \tag{2.7}$$

where R_{mn} is the reflection matrix, and its elements are determined by the coupling of each incident harmonic, F_n, with the entire manifold of scattered ones, D_m. Let us now demonstrate this method for a surface whose geometry enables relatively simple expressions.

2. The reflection matrix of a rectangular grating

We consider a metallic grating made of a very-high-conductivity material, so that the tangential electric field vanishes on its surface. In each cell there is a groove of a length $L-d$ and a height a, as described in Fig. 2. The EM field in the Mth cell ($ML+d < x < ML+L$ and $-a < z < 0$) is given by

$$H_y^{(M)} = H_0 \sum_{s=0}^{\infty} A_s^{(M)} \cos[q_s(x - x_M)] \cos[Q_s(z+a)] \ , \tag{2.8}$$

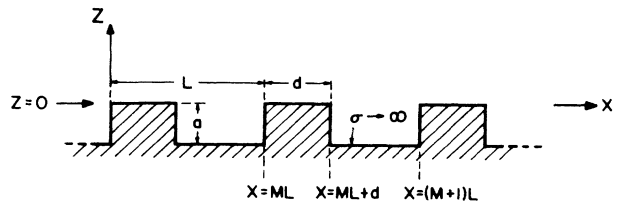

FIG. 2. The geometry used to demonstrate the calculation of the reflection matrix: L is the grating periodicity, a is the groove height, and $L-d$ is its length.

where

$$q_s=\frac{\pi s}{L-d},\quad Q_s=\left[\frac{\omega^2}{c^2}-q_s^2\right]^{1/2},\quad x_M=ML+d\ .$$

Above the grating, the field is described by the expressions of Eqs. (2.3) and (2.6). The amplitudes $D_m(k)$ and $A_s^{(M)}$ (where ω is omitted for convenience) should be determined by imposing the boundary conditions at $z=0$. Continuity of the tangential component of the magnetic field at $z=0$ and $ML+d\le x\le(M+1)L$ implies

$$\sum_{m=-\infty}^{\infty}\int_{-\pi/L}^{\pi/L}dk(F_m+D_m)e^{-jk_m x}=\sum_{s=0}^{\infty}A_s^{(M)}\cos[q_s(x-x_M)]\cos(Q_s a)\ . \tag{2.9}$$

The functions $\cos[q_s(x-x_M)]$ are orthogonal to each other in the domain where Eq. (2.9) is defined, and the amplitude $A_s^{(M)}$ can therefore be expressed as

$$A_s^{(M)}=\frac{1}{g_s\cos(Q_s a)}\times\sum_{m-\infty}^{\infty}\int_{-\pi/L}^{\pi/L}dk(F_m+D_m)e^{-jkML}\mathcal{L}(k_m;s) \tag{2.10}$$

with $g_0=1$, $g_{s\neq 0}=\frac{1}{2}$, $\mathcal{L}(k_m;s)$ given by

$$\mathcal{L}(k_m;s)=e^{-jk_m d}\frac{1}{2}\left[e^{-j\theta_-}\frac{\sin\theta_-}{\theta_-}+e^{-j\theta_+}\frac{\sin\theta_+}{\theta_+}\right]$$

and $\theta_\pm=\frac{1}{2}[k_m(L-d)\pm\pi s]$.

The tangential component of the electric field is readily derived from Maxwell equations, i.e., $j\omega\epsilon_0 E_x=-\partial H_y/\partial z$; continuity of the tangential component of the electric field at $z=0$ implies

$$\sum_{m-\infty}^{\infty}\int_{-\pi/L}^{\pi/L}dk\frac{\beta_m}{j\omega/c}(F_m-D_m)e^{-jk_m x}=\begin{cases}0 & \text{for } ML\le x\le ML+d\\ \sum_s A_s^{(M)}\left[\dfrac{-Q_s}{j\omega/c}\right]\cos[q_s(x-x_M)]\sin(Q_s a) & \text{for } ML+d\le x\le(M+1)L.\end{cases} \tag{2.11}$$

Equation (2.10) is now substituted in Eq. (2.11), the resulting expression is multiplied by e^{jKx}, and intergrated over the entire domain ($-\infty<x<\infty$). The result can be written as

$$F_m(\omega,k)-D_m(\omega,k)=\sum_{n=-\infty}^{\infty}Z_{mn}(\omega,k)[F_n(\omega,k)+D_n(\omega,k)]\ , \tag{2.12}$$

where

$$Z_{mn}(\omega,k)=-\frac{L-d}{L}\frac{1}{\beta_n}\sum_s\frac{Q_s\tan(Q_s a)}{g_s}\times\mathcal{L}(k_n;s)\mathcal{L}^*(k_m;s)$$

is the impedance matrix. Adopting a vector notation for $F_n(\omega,k)$ and $D_m(\omega,k)$, Eq. (2.7) reads

$$\mathbf{D}=\underline{R}\mathbf{F}\ ,$$

so that the reflection matrix is given in terms of the impedance matrix by

$$\underline{R}\equiv(\underline{I}+\underline{Z})^{-1}(\underline{I}-\underline{Z})\ . \tag{2.13}$$

Although $\underline{Z}$ is expressed in terms of analytical functions, evaluation of $\underline{R}$ is possible only numerically—after a suitable inversion of the matrix, $\underline{I}+\underline{Z}$, and multiplication by $\underline{I}-\underline{Z}$.

For more complex geometries, the calculations become more complicated, and usually the numerical effort is significant. This is practically the reason we choose to represent the scattering process by means of a reflection matrix, as it separates the numerical part of the calculation of the boundary condition problem, and the essence of the physical picture. Exact evaluation of $\underline{R}$ is not always necessary, since experiments can be performed to measure some of these matrix elements. The entire group of reflection matrix elements which couple between incident and scattered propagating harmonics, can be established by a series of simple experiments. In such experiments a plane propagating wave, e.g., as described by Eq. (2.5), impinges on the grating, and the measured reflected waves determine the corresponding reflection matrix elements, i.e.,

$$R_{mN}(\omega,k_0)=D_m(\omega,k_0)\ . \tag{2.14}$$

Another group of the reflection matrix terms can be measured using the Smith-Purcell effect. In this case it is possible to find these terms which couple incident *evanescent*

waves and outgoing *propagating* ones. To this end we reformulate the Smith-Purcell effect in Sec. II B 3, in terms of the reflection matrix.

3. *Smith-Purcell radiation*

Let us consider a charged line $\bar{q}$, which moves at a height h above and parallel to the grating with a constant velocity $\mathbf{V}=V_0\mathbf{1}_x$, as described in Fig. 3. The field of this charged line is seen in the laboratory frame of reference as evanescent waves, some of which are moving towards the corrugated surface. This field can be expressed as a superposition of plane waves of different frequencies, thus the incident wave in the domain $z<h$ can be expressed as

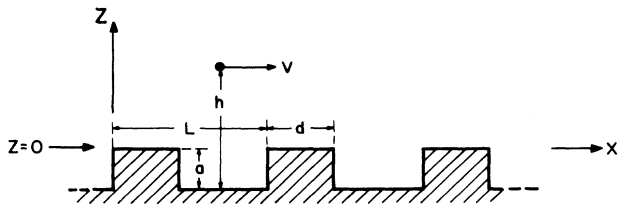

FIG. 3. A charged line which moves uniformly above a corrugated surface is used for the description of Smith-Purcell effect.

$$H_y^{(\mathrm{inc})}(x,z,t)=2\,\mathrm{Re}\left[\int_0^\infty d\omega\, e^{j\omega t}\sum_{m=-\infty}^{\infty}\int_{-\pi/L}^{\pi/L}dk\,\bar{F}_m(k,\omega)e^{-jk_m x}e^{\beta_m z}\right]. \tag{2.15}$$

If $H^{(\mathrm{inc})}$ is calculated for a charged line in empty space, the amplitudes $\bar{F}_m(k,\omega)$ are given by

$$\bar{F}_m(\omega,k)=\bar{F}(\omega,k_x=k_m)=\frac{H_1}{2\gamma}\delta(\omega-\beta ck_x)h\exp\left[jx_0'\gamma\left[k_x-\beta\frac{\omega}{c}\right]\right]\exp\left[-\gamma h\left|k_x-\beta\frac{\omega}{c}\right|\right], \tag{2.16}$$

where $H_1=\beta\gamma(1/\eta_0)(\bar{q}/2\pi\epsilon_0)(2/h)$, $\beta=V_0/c$, $\gamma=1/(1-\beta^2)^{1/2}$, and x_0' is the position of the charged line in its rest frame of reference. Similarly, we can write the scattered wave as a superposition of plane waves, namely,

$$H_y^{(\mathrm{sc})}(x,z,t)=2\,\mathrm{Re}\left[\int_0^\infty d\omega\, e^{j\omega t}\sum_{m'=-\infty}^{\infty}\int_{-\pi/L}^{\pi/L}dk\,D_{m'}(k,\omega)e^{-jk_{m'}x-\beta_{m'}z}\right]. \tag{2.17}$$

Remember that m' labels the outgoing harmonics while m labels the incoming ones.

According to the definition of the reflection matrix, the scattered wave is given by

$$H_y^{(\mathrm{sc})}(x,z,t)=2\,\mathrm{Re}\left[\int_0^\infty d\omega\, e^{j\omega t}\sum_{m'=-\infty}^{\infty}\int_{-\pi/L}^{\pi/L}dk\left[\sum_{m=-\infty}^{\infty}R_{m'm}(\omega,k)\bar{F}_m(\omega,k)\right]e^{-jk_{m'}x-\beta_{m'}z}\right]. \tag{2.18}$$

It should be emphasized that here we took advantage of the fact that the reflection matrix couples only harmonics with the same k, the wave vector in the first Brillouin zone. The last equation is the formal expression for the scattered wave; in what follows we shall analyze the relevant terms of this field.

Far away from the grating, only propagating harmonics are detectable; thus we replace the infinite summation over m' by a summation $\sum_m'$ over the radiating harmonics only. This condition can be mathematically formulated in terms of the harmonics indexes m', which obey the following inequality:

$$\frac{\omega}{c}>\left|k+\frac{2\pi}{L}m'\right|. \tag{2.19}$$

The summation over m is also limited due to the Dirac δ function in $\bar{F}_m(\omega,k)$ of Eq. (2.16), which in our notation reads

$$\delta\left[\omega-\beta c\left[k+\frac{2\pi}{L}m\right]\right]=\frac{1}{\beta c}\delta\left[\frac{\omega}{c}\frac{1}{\beta}-k_m\right]. \tag{2.20}$$

The interpretation of this expression is simple: For a given velocity β, the frequency ω determines k and m through

$$\frac{\omega}{c}\frac{1}{\beta}=k+\frac{2\pi}{L}m. \tag{2.21}$$

The integration over k can now be carried out, using Eq. (2.20) and bearing in mind that m is connected to ω through Eq. (2.21). The resulting scattered wave is given by

$$H_y^{(\mathrm{sc})}(x,z,t)=\frac{H_1 h}{2\gamma\beta c}2\,\mathrm{Re}\left[\int_0^\infty d\omega\exp\left[-\frac{\omega}{c}\frac{h}{\gamma\beta}\right]\exp\left[jx_0'\frac{\omega}{c\gamma\beta}\right]\times\left\{\sum_{m'}{}'R_{m'm}(k,\omega)e^{+j\omega t-jk_{m'}x}\exp\left[-jz\left[\frac{\omega^2}{c^2}-k_{m'}^2\right]^{1/2}\right]\right\}_{k=\omega/V_0-2\pi/L_m}\right]. \tag{2.22}$$

Far away from the grating, the propagating components of this field are measured by a detector whose angle with the z axis is Θ_D. The x component of a propagating wave is therefore $k_x=(\omega/c)\sin\Theta_D$, or in our notation

$$\frac{\omega}{c}\sin\Theta_D=k+\frac{2\pi}{L}m' . \tag{2.23}$$

We now turn to the question of which frequencies are detected within a given angle by this detector. If we express ω, using Eqs. (2.21) and (2.23), as a function of m and m', namely,

$$\frac{\omega}{c}=\frac{2\pi}{L}\frac{m-m'}{1/\beta-\sin\Theta_D} , \tag{2.24}$$

the problem is not yet solved, since from Eq. (2.21) it is obvious that m is a function of ω. However, bearing in mind that ω is a positive quantity we conclude from the last expression that

$$m>m' . \tag{2.25}$$

Instead of Eq. (2.24), let us express k as a function of m and m'. This can be done by substituting Eq. (2.24) in Eq. (2.21) or Eq. (2.23), yielding

$$k\frac{L}{2\pi}=\frac{m\beta\sin\Theta_D-m'}{1-\beta\sin\Theta_D} . \tag{2.26}$$

Bearing in mind that k is defined only in the first Brillouin zone, Eq. (2.26) provides the selection criterion for m and m', hence

$$-\frac{1}{2}<\frac{m\beta\sin\Theta_D-m'}{1-\beta\sin\Theta_D}<\frac{1}{2} . \tag{2.27}$$

The shaded area in Fig. 4 describes the region where m and m' might be found. Theoretically, for given β and Θ_D there is an infinite number of pairs $\{m,m'\}$ within this region, but recalling Eq. (2.22) we realize that the exponent $\exp[-(\omega/c)(h/\gamma\beta)]$ "cuts off" the contribution of the higher frequencies; therefore if $(\omega/c)(h/\gamma\beta)>20$, then the radiation amplitude can be considered for all practical purposes negligible. Now, substituting the last expression in Eq. (2.21) and neglecting $kL/2\pi$ relative to $m_{\max}$, we can define an upper limit value of the incident harmonic index which still has a non-negligible contribution to the outgoing radiating harmonic:

$$m_{\max}=1+\text{int}\left[\frac{20}{2\pi}\frac{L}{h}\gamma\right] . \tag{2.28}$$

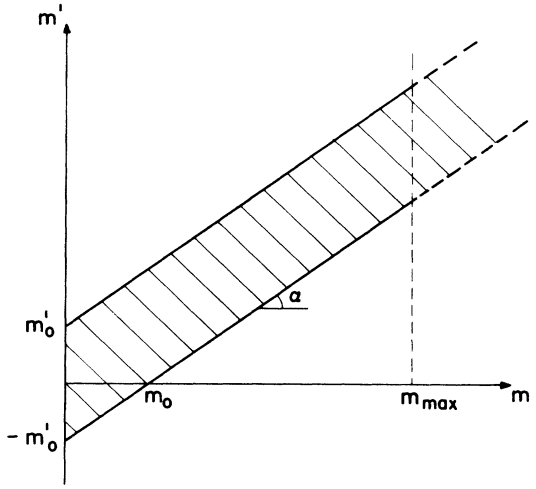

FIG. 4. The participating harmonics. The shaded area determines the range of harmonics ($[m,m']$) which participate in the scattering process. The slope of both lines is $\alpha=\tan^{-1}(\beta\sin\theta)$, $m'_0=\frac{1}{2}(1-\beta\sin\Theta_D)$, and $m_0=\frac{1}{2}(1-\beta\sin\Theta_D)/(\beta\sin\Theta_D)$. $m_{\max}$ is the maximum value of m which has a significant contribution to the scattering process.

The role of this supremum is also geometrically presented in Fig. 4. The group of m and m' which solve Eqs. (2.25), (2.27), and (2.28) denoted by $[m,m']$, is the answer to the question asked above. In Tables I and II we bring a numerical example of the possible values of $\Omega_1=(\omega/c)(L/2\pi)$, $\Omega_2=(\omega/c)(1/\beta)(h/\gamma)$, m, and m' for different angles Θ_D, velocities β; the height parameter is assumed to be $2\pi h/L=\pi$.

Next we ask what is the field at the detector? The answer is rather obvious since the intergration over ω in Eq. (2.22) can be replaced by summation over the possible m's as follows:

$$H_1\frac{h}{2\gamma\beta c}2\,\text{Re}\left[\int_0^\infty d\omega\sum_{m'}'(\cdot)\right]$$
$$=H_1\frac{h}{2\gamma\beta c}2\,\text{Re}\left[\frac{2\pi}{L}c\frac{1}{1/\beta-\sin\theta}\sum_{[m,m']}(\cdot)\right] ,$$

and substituting the explicit expression for H_1, the scattering wave reads

$$H_y^{(\text{sc})}=\frac{\bar{q}c/L}{1/\beta-\sin\Theta_D}2\,\text{Re}\left[\sum_{[m,m']}\exp\left[-\omega_{mm'}\frac{h}{\gamma\beta c}+jx'_0\frac{\omega_{mm'}}{\gamma\beta c}\right]R_{m'm}(k_{mm'},\omega_{mm'})\right.$$
$$\left.\times\exp\left[j\omega_{mm'}t-jx\frac{\omega_{mm'}}{c}\sin\Theta_D-jz\frac{\omega_{mm'}}{c}\cos\Theta_D\right]\right] , \tag{2.29}$$

where

$$\omega_{mm'}=\frac{2\pi}{L}c\frac{m-m'}{1/\beta-\sin\Theta_D},\quad k_{mm'}=\frac{2\pi}{L}\frac{m\beta\sin\Theta_D-m'}{1-\beta\sin\Theta_D} . \tag{2.30}$$

TABLE I. The participating harmonics in the Smith-Purcell effect; the first contribution, i.e., $n=m'-m=-1$. At each angle θ of detection we calculate the frequency which corresponds to three different electron velocities. The exponential decay due to beam height above the grating is also determined. As the radiation gets closer to the beam direction, the frequency increases and the exponential decay gets larger. Notice that the labels of the participating harmonics increase too. $x[y]=x\times 10^{y}$.

θ	β	m	m'	$Q=q\frac{L}{2\pi}$	$\Omega_1=\frac{\omega}{c}\frac{L}{2\pi}$	$\Omega_2=\frac{\omega}{c}\frac{h}{\gamma\beta}$	$e^{-2\Omega_2}$
−90°	1/4	1	0	−0.200	0.200	2.433	0.770[−2]
	$1/\sqrt{2}$	1	0	−0.414	0.414	1.301	0.741[−1]
	0.9	1	0	−0.474	0.474	0.721	0.236[0]
−60°	1/4	1	0	−0.178	0.206	2.500	0.674[−2]
	$1/\sqrt{2}$	1	0	−0.380	0.439	1.378	0.635[−1]
	0.9	1	0	−0.438	0.506	0.770	0.214[0]
−30°	1/4	1	0	−0.111	0.222	2.704	0.448[−2]
	$1/\sqrt{2}$	1	0	−0.261	0.522	1.641	0.375[−1]
	0.9	1	0	−0.310	0.621	0.944	0.151[0]
0°	1/4	1	0	0.000	0.250	3.042	0.228[−2]
	$1/\sqrt{2}$	1	0	0.000	0.707	2.221	0.118[−1]
	0.9	1	0	0.000	0.900	1.369	0.647[−1]
30°	1/4	1	0	0.143	0.286	3.476	0.956[−3]
	$1/\sqrt{2}$	2	1	−0.453	1.094	3.436	0.104[−2]
	0.9	2	1	−0.182	1.636	2.490	0.687[−2]
60°	1/4	1	0	0.276	0.319	3.882	0.425[−3]
	$1/\sqrt{2}$	3	2	−0.420	1.824	5.731	0.105[−4]
	0.9	5	4	−0.466	4.080	6.208	0.405[−5]
90°	1/4	1	0	0.333	0.333	4.056	0.300[−3]
	$1/\sqrt{2}$	3	2	0.414	2.414	7.584	0.258[−6]
	0.9	10	9	0.000	9.000	13.694	0.127[−11]

The exponential factor in Eq. (2.29) implies that practically, only the first term $n=m'-m=-1$ has a nonzero contribution to the radiation process and therefore only one term of $\underline{R}$ is significant.

With the EM field determined for an infinite grating, it is possible to evaluate the average power emitted by a charged beam which moves above a finite grating of length D. We wish to emphasize that in what follows we neglect fringe effects, therefore D is considered much larger than all other lengths that have been introduced before; however, it is still much smaller than the distance (r) between the grating and the detector. The normalized power density emitted in the interval between Θ_D and $\Theta_D+d\Theta$ by a very thin beam is given by

$$\bar{s}\equiv\frac{S_r}{\left[2\pi^2\frac{\Phi_0 I}{2\pi r\Delta_y}\left(\frac{D}{L}\right)^3\right]}=\frac{\cos^2\Theta_D}{(1/\beta-\sin\Theta_D)^2}\times\sum_{[m,m']}(m-m')|R_{m'm}|^2\exp\left[-2\frac{\omega_{mm'}}{c}\frac{h}{\gamma\beta}\right],\tag{2.31}$$

where I is the total current injected, $\Phi_0=\bar{q}/2\pi\epsilon_0$, and Δ_y is the device width (y direction). For a beam of thickness Δ the expression for $\bar{s}$ reads

$$\bar{s}=\frac{\cos^2\Theta_D}{(1/\beta-\sin\Theta_D)^2}\times\sum_{[m,m']}(m-m')|R_{m'm}|^2\exp\left[-2\frac{\omega_{mm'}}{c}\frac{h}{\gamma\beta}\right]\times\exp\left[-\frac{\omega_{mm'}}{c}\frac{\Delta}{\gamma\beta}\right]\times\left\{\frac{\left[\sinh\left[\frac{\omega_{mm'}}{c}\frac{\Delta}{\gamma\beta}\right]\right]}{\left[\frac{\omega_{mm'}}{c}\frac{\Delta}{\gamma\beta}\right]}\right\}.\tag{2.32}$$

A similar result was obtained by Gover *et al.*[18] using van den Berg's method;[19–21] this was also verified in Ref. 18 in particular for large Δ. Using one of these two expressions it is possible to determine $|R_{m'm}|$ by a simple Smith-Purcell experiment.

We wish to reemphasize that the reflection matrix is, at this stage, only a convenient way to represent the boundary conditions at the grating. A numerical calculation is unavoidable for a given grating as could be concluded

TABLE II. The second contribution, i.e., $n=m'-m=-2$, of the participating harmonics $[m,m']$. At each angle θ of detection we calculate the frequency corresponding to three different electron velocities; this frequency is higher than the first contribution (see Table I). The exponential decay due to beam height above the grating is also determined and it is found to be much stronger than for $n=-1$. Notice that at the same velocity and angle (as close as possible to $\theta=90°$) two different harmonics participate. For example, at $\theta=90°$ for $\beta=\frac{1}{4}$ in the case that $n=-1$ the [1,0] harmonics participate whereas when $n=-2$ the harmonics labels are [3,1]. $x[y]=x\times 10^{y}$.

θ	β	m	m'	$Q=k\frac{L}{2\pi}$	$\Omega_1=\frac{\omega}{c}\frac{L}{2\pi}$	$\Omega_2=\frac{\omega}{c}\frac{h}{\gamma\beta}$	$e^{-2\Omega_2}$
−90°	1/4	2	0	−0.400	0.400	4.867	0.592[−4]
	$1/\sqrt{2}$	1	−1	0.176	0.828	2.603	0.548[−2]
	0.9	1	−1	0.053	0.947	1.441	0.560[−1]
−60°	1/4	2	0	−0.356	0.411	5.001	0.453[−4]
	$1/\sqrt{2}$	1	−1	0.240	0.877	2.755	0.405[−2]
	0.9	1	−1	0.124	1.012	1.539	0.461[−1]
−30°	1/4	2	0	−0.222	0.444	5.408	0.201[−4]
	$1/\sqrt{2}$	1	−1	0.477	1.045	3.282	0.141[−2]
	0.9	1	−1	0.379	1.241	1.889	0.229[−1]
0°	1/4	2	0	0.000	0.500	6.084	0.519[−5]
	$1/\sqrt{2}$	2	0	0.000	1.414	4.443	0.138[−3]
	0.9	2	0	0.000	1.800	2.739	0.418[−2]
30°	1/4	2	0	0.286	0.571	6.953	0.913[−6]
	$1/\sqrt{2}$	3	1	0.094	2.188	6.873	0.107[−5]
	0.9	4	2	−0.364	3.273	4.980	0.473[−4]
60°	1/4	3	1	−0.447	0.638	7.765	0.180[−6]
	$1/\sqrt{2}$	5	3	0.160	3.648	11.462	0.111[−9]
	0.9	9	7	0.067	8.160	12.416	0.164[−10]
90°	1/4	3	1	−0.333	0.667	8.112	0.900[−7]
	$1/\sqrt{2}$	7	5	−0.172	9.828	15.169	0.667[−13]

from van den Berg's works.[19–21] This convenient formulation enables us to show that although the spectrum of the source, as expressed in Eq. (2.15), is continuous, the spectrum of the EM radiation as measured by the detector is *discrete*. This result is in accordance with the Smith-Purcell experiment. The kinematic aspect of this filtering process was determined by Eqs. (2.19), (2.21), and (2.23) together with the definition of k.

C. Electron dynamics

For a solution of Eq. (2.1) we have just introduced a convenient way to describe the boundary conditions. In this section the source term of this equation is determined by employing the fluid approximation to calculate the electron dynamics. Within this approximation we tacitly assume that the beam temperature is zero; the effect of the temperature on FEL's performance has been already investigated by Gover and Yariv.[22]

The velocity field $\mathbf{V}$ consists of two terms, the average velocity field $V_0\mathbf{1}_x$, and a small disturbance $U_x(x,z,t)$, due to the presence of a weak electric field, i.e., $|U_x|\ll V_0$. This disturbance is determined by the linearized equation of motion

$$m\gamma^3\frac{d}{dt}U_x(x,z,t)=-eE_x(x,z,t)\ . \tag{2.33}$$

The density field n, similarly, has its average value n_0 and a small disturbance $n_1(x,z,t)$ where $|n_1|\ll n_0$. This quantity is in turn related to the velocity field through the linearized continuity equation

$$\frac{\partial}{\partial t}n_1(x,z,t)+\frac{\partial}{\partial x}[V_0n_1(x,z,t)+U_x(x,z,t)n_0]=0\ . \tag{2.34}$$

Solving the last two equations for U_x and n_1 in terms of the electric field, we can determine the current density that this field induces through

$$J_x(x,z,t)=-e[n_0U_x(x,z,t)+n_1(x,z,t)V_0]\ . \tag{2.35}$$

As was mentioned in the Introduction we neglect transients in time and in space. The Floquet-Bloch notation

$$G_x(x,z,t)=\mathrm{Re}\left[e^{j\omega t}\sum_{s=-\infty}^{\infty}\int_{-\pi/L}^{\pi/L}dk\,\tilde{G}_{x,s}(k,z,\omega)e^{-jk_sx}\right] \tag{2.36}$$

is adopted to describe the electric field $E_x(x,z,t)$, the current $J_x(x,z,t)$, the velocity $U_x(x,z,t)$, and the density $n_1(x,z,t)$ in terms of the corresponding amplitudes $\tilde{E}_{x,s}(k,z,\omega)$, $\tilde{J}_{x,s}(k,z,\omega)$, $\tilde{U}_{x,s}(k,z,\omega)$, and $\tilde{n}_{1,s}(k,z,\omega)$. If we employ Eq. (2.36) we can eliminate $\tilde{n}$ and $\tilde{U}$ so that

the current amplitude reads

$$\tilde{J}_{x,s}(k,z,\omega)=-j\omega\epsilon_0\frac{\omega_p^2}{\gamma^2(\omega-V_0k_s)^2}\tilde{E}_{x,s}(k,z,\omega)\ , \quad (2.37)$$

where $\omega_p=(e^2n_0/\epsilon_0m\gamma)^{1/2}$ is the plasma frequency. This frequency is by many orders of magnitude smaller than the electric field characteristic frequency and the induced current is non-negligible only near resonance, i.e., when $\omega\sim V_0k_M$ where M is defined by

$$\frac{\omega}{V_0}\equiv\tilde{k}+\frac{2\pi}{L}M\ . \quad (2.38)$$

In the rest of this work we neglect even the currents which correspond to "neighbor" harmonics, such as $M+1$ and $M-1$. The harmonic M whose corresponding current has the greatest amplitude (thus the largest influence) is called the synchronous harmonic (SH) or synchronous wave (SW). We are now in a position to solve Eq. (2.1) systematically.

III. THE AMPLIFIER

A. The solution of the electromagnetic problem

In order to solve the electromagnetic problem as described by the configuration of Fig. 1, the upper half plane, $z>0$, is divided into three domains. Above the beam $z\geq h+\Delta$, we have an incident radiation field which is described by Eq. (2.3) and the scattered field described by an expression similar to Eq. (2.6). Within the beam, $h\leq z\leq h+\Delta$, the y component of the magnetic field is a self-consistent solution of the differential equation, Eq. (2.1), together with the current density of Eq. (2.37), i.e.,

$$\left[\frac{d^2}{dz^2}-k_m^2+\frac{\omega^2}{c^2}\right]\tilde{H}_{y,m}(k,z,\omega)$$
$$=j\omega\epsilon_0\frac{\omega_p^2}{\gamma^2(\omega-V_0k_m)^2}\frac{d}{dz}\tilde{E}_{x,m}(k,z,\omega)\ , \quad (3.1)$$

where $\tilde{H}_{y,m}(k,z,\omega)$ is the amplitude of the magnetic field [see Eq. (2.36)]. $\tilde{H}_{y,m}$ and $\tilde{E}_{x,m}$ are also related by

$$-j\omega\mu_0\tilde{H}_{y,m}(k,z,\omega)$$
$$=-\left[-jk_m\tilde{E}_{z,m}(k,z,\omega)-\frac{d}{dz}\tilde{E}_{x,m}(k,z,\omega)\right] \quad (3.2)$$

and

$$j\omega\epsilon_0\tilde{E}_{z,m}(k,z,\omega)=-jk_m\tilde{H}_{y,m}(k,z,\omega)\ ; \quad (3.3)$$

substituting Eq. (3.3) in Eq. (3.2) we get

$$\frac{d\tilde{E}_{x,m}(k,z,\omega)}{dz}=-j\omega\mu_0\left[\frac{\omega^2/c^2-k_m^2}{\omega^2/c^2}\right]\tilde{H}_{y,m}(k,z,\omega)\ . \quad (3.4)$$

The general solution of Eqs. (3.1) and (3.4) is

$$H_y(x,z,t)=\mathrm{Re}\left[e^{j\omega t}\sum_{m=-\infty}^{\infty}\int_{-\pi/L}^{\pi/L}dk\,e^{-jk_mx}(A_me^{-j\alpha_mz}+B_me^{j\alpha_mz})\right]\ , \quad (3.5)$$

where

$$\alpha_m^2=-\beta_m^2\left[1-\frac{\omega_p^2}{\gamma^2(\omega-V_0k_m)^2}\right]$$

and A_m, B_m will be determined by the boundary conditions. We wish to emphasize that the divergence of **E** is not assumed here to be negligible (as in Ref. 4).

Between the beam and the grating, there is a gap of height h and the wave equation in this region ($0\leq z\leq h$) is homogeneous. Exploiting the definition of the surface reflection matrix $\underline{R}$, we can write the field in this third region as follows:

$$H_y(x,z,t)=\mathrm{Re}\left\{e^{j\omega t}\sum_{m=-\infty}^{\infty}\int_{-\pi/L}^{\pi/L}dk\,e^{-jk_mx}\left[S_me^{\beta_mz}+e^{-\beta_mz}\left[\sum_{n=-\infty}^{\infty}R_{mn}S_n\right]\right]\right\}\ . \quad (3.6)$$

The four amplitudes D_m, A_m, B_m, and S_m of the mth harmonic are determined by imposing the continuity of the tangential components of the EM field at the interface of the beam with the vacuum (i.e., at $z=h$ and $z=h+\Delta$). Extracting the amplitude of the scattered wave (D_m) we find that

$$D_m=\sum_{n=-\infty}^{\infty}\left[R_{mn}+R_{mM}\frac{1}{1/U_M-R_{MM}}R_{Mn}\right]F_n\ , \quad (3.7)$$

where the beam and the air gap influence are expressed through

$$U_M=e^{-2\beta_Mh}\frac{(\beta_M^2+\alpha_M^2)\sin(\alpha_M\Delta)}{2\alpha_M\beta_M\cos(\alpha_M\Delta)+(\beta_M^2-\alpha_M^2)\sin(\alpha_M\Delta)}\ . \quad (3.8)$$

Equation (3.7) is our result for the response function. Notice that the first term of Eq. (3.7) is the bare scattering of the incoming wave by the grating. The second term, which is the beam contribution to the scattered waves, is our main concern here, and it is easily interpreted as follows: R_{Mn} transforms part of the incident wave F_n into the synchronous evanescent wave M; the latter is

then amplified (or attenuated) by the beam as indicated by the factor $1/(1/U_M - R_{MM})$ and then transformed back, by R_{mM}, into the enhanced scattered wave.

An additional physical insight into the second term in Eq. (3.7) can be achieved if we expand the denominator for $|U_M R_{MM}| < 1$ as a geometrical series, i.e.,

$$R_{mM}\frac{1}{1/U_M - R_{MM}}R_{Mn} = R_{mM}U_M\left[\sum_{p=0}^{\infty}(R_{MM}U_M)^p\right]R_{Mn} \quad (3.9)$$

or explicitly, the right-hand side reads as

$$R_{mM}U_M R_{Mn} + R_{mM}U_M R_{MM}U_M R_{Mn} + R_{mM}U_M R_{MM}U_M R_{MM}U_M R_{Mn} + \cdots .$$

This expression describes an infinite reflection process between the beam (U_M) and the grating (R_{MM}). the first term in this series is interpreted as follows: part of the incident wave amplitude F_n is "transformed" by the grating R_{Mn} into an evanescent synchronous wave M. The amplitude of this wave decreases exponentially [$\exp(-\beta_M h)$] when it reaches the beam; there, the amplitude is changed and the wave is reflected towards the grating. Along its way in the gap, the amplitude decays by another factor of $\exp(-\beta_M h)$. This fate of the wave is described by U_M. When it reaches the grating, a part, R_{mM}, of the SW is scattered: this is the $p=0$ contribution (see Fig. 5). Reading the second term from right to left, we realize that the first three terms describe the same process as above, except that in the last reflection process the synchronous wave is reflected back into itself, i.e., R_{mM} is replaced by R_{MM}. This can be considered as a new SW which undergoes an identical process as previously: the influence of the gap and the beam is described by U_M and again, a part of this wave, R_{mM}, is reflected by the grating; this is the $p=1$ contribution. The other terms of the series can be interpreted similarly. This infinite process is described diagrammatically in Fig. 5.

B. The poles of the response function

We are now in a position to analyze the poles of the response function of the SP amplifier. The analytical continuation of the denominator of Eq. (3.7) into the complex k plane enables us to find the poles of the response function, i.e., the solutions of

$$\frac{1}{U_M} - R_{MM} = 0 . \quad (3.10)$$

Here U_M characterizes the beam and the air gap influence, whereas R_{MM} corresponds to the reflection coefficient of the resonating evanescent harmonic from the grating. Obviously $R_{MM}(k,\omega)$ would vary from surface to surface. However, close to resonance, when $k_M \simeq k_e \equiv \omega/V_0$, we expect R_{MM} to behave essentially the same for all surfaces that can *support* the harmonic M. Since Eq. (3.10) depends on a *single diagonal* term of the reflection matrix we employ a simple model in order to find an explicit expression for R_{MM} near resonance. We model the surface as made of a dielectric (ϵ) slab of thickness d on top of an ideal conductor (see Fig. 6); the parameters ϵ and d are chosen to support the evanescent harmonic M. The reflection matrix of this system is diagonal, and the term which corresponds to R_{MM} is then found to be

$$R_{MM} = \frac{\beta_M - (\beta_D/\epsilon)\tanh(\beta_D d)}{\beta_M + (\beta_D/\epsilon)\tanh(\beta_D d)} , \quad (3.11)$$

where $\beta_D = [k_M^2 - \epsilon(\omega/c)^2]^{1/2}$. The condition that this system of ϵ and d will support a slow wave of a frequency ω and wave vector $k_M = k_x = \omega/V_0$ is satisfied if these parameters obey the following relation:

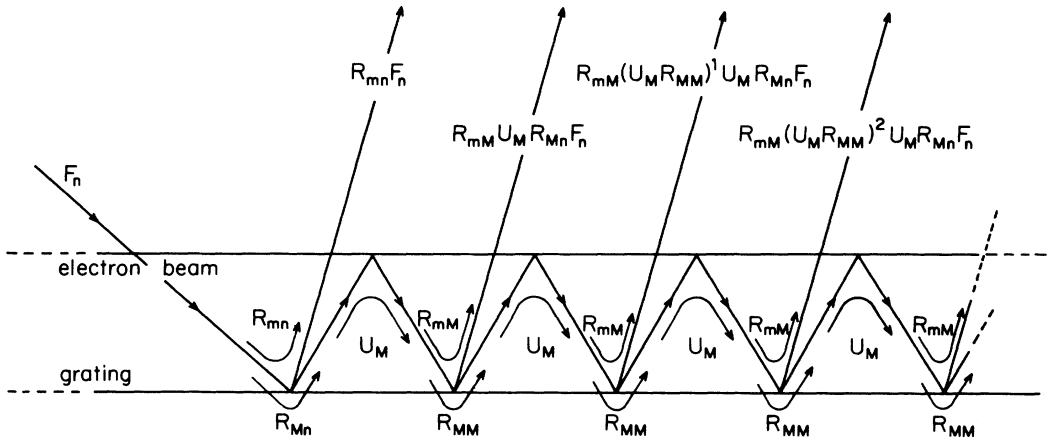

FIG. 5. The infinite reflection process between the grating and the beam. The beam is transparent to the incident (propagating) wave which is reflected by the grating ($R_{mn}F_n$). The beam does not affect these waves, except the synchronous wave (M) which is partially scattered back towards the grating (U_M). At the grating, this wave is again reflected $R_{mM}U_M R_{Mn}F_n$, and as previously the beam does not affect these waves except the synchronous one ($m=M$). Notice the important role played by the diagonal reflection matrix term which corresponds to the synchronous wave.

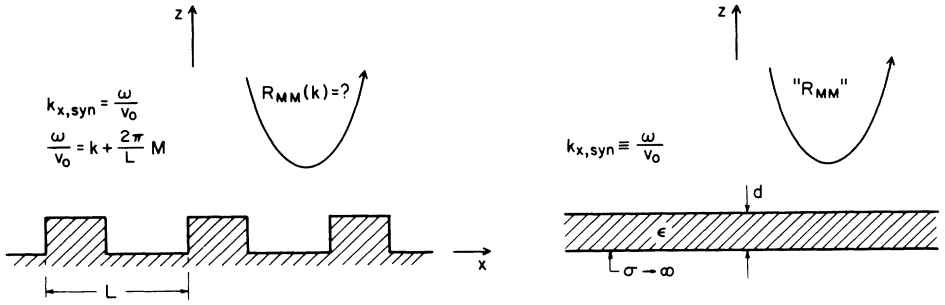

FIG. 6. A model for calculating R_{MM} near resonance.

$$\beta_M^{(0)} + (\beta_D^{(0)}/\epsilon)\tanh(\beta_D^{(0)} d) = 0 , \tag{3.12}$$

where the superscript (0) indicates that no beam is present. We now compare the left-hand side of Eq. (3.12) with the denominator of the reflection coefficient, Eq. (3.11). We realize that the condition for the slow wave system to support the synchronous wave is equivalent to the requirement that the reflection coefficient is singular or that it has a resonance. A graphic solution of Eq. (3.12) is illustrated in Fig. 7. In the presence of the beam we expect a small deviation, q, from resonance, ω/V_0, and therefore we substitute

$$k_M = k_e + q, \quad |q| \ll \omega/V_0 , \tag{3.13}$$

into Eq. (3.11), and find that it can be cast into the form

$$R_{MM} = \frac{2k_e/\gamma^2}{q} \bar{Q} , \tag{3.14}$$

where $\bar{Q}$ depends on the parameters of the surface, and is of order unity. The $\bar{Q}$ which corresponds to our particular model is given by

$$\bar{Q} = \left[1 + \frac{1}{\gamma^2(\epsilon\beta^2 - 1)} + \frac{\omega}{c} d \frac{1}{\epsilon\beta\gamma^3} \frac{\epsilon^2 + \gamma^2(\epsilon\beta^2 - 1)}{(\epsilon\beta^2 - 1)^{3/2}} \right]^{-1}$$

and is plotted versus the dielectric coefficient in Fig. 8. We observe that, indeed, it is a very slowly varying function of ϵ, the model's "degree of freedom."

Next we return to Eq. (3.10), substitute Eq. (3.14) for R_{MM}, and Eq. (3.13) for the wave number q, and find

$$q^3 = -\frac{\omega_p^2}{V_0^2} \frac{k_e}{\gamma^4} \frac{e^{-2\eta}\sinh(\tau\delta)}{\tau\cosh(\tau\delta) + \frac{1}{2}(1+\tau^2)\sinh(\tau\delta)} \bar{Q} , \tag{3.15}$$

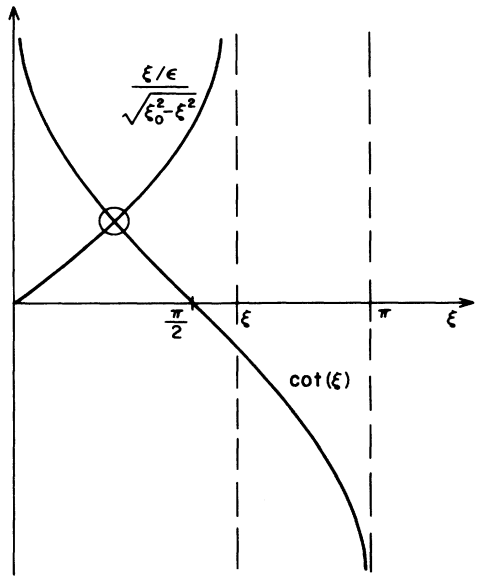

FIG. 7. A graphic solution of Eq. (3.12). We defined here $\xi = \beta_D^{(0)} d$ and $\xi_0 = \sqrt{\epsilon - 1}(\omega/c)d$ so that Eq. (3.12) reads $\cot(\xi) = (\xi/\epsilon)/(\xi_0^2 - \xi^2)^{1/2}$. The solution corresponds to the case that ξ_0 is smaller than π.

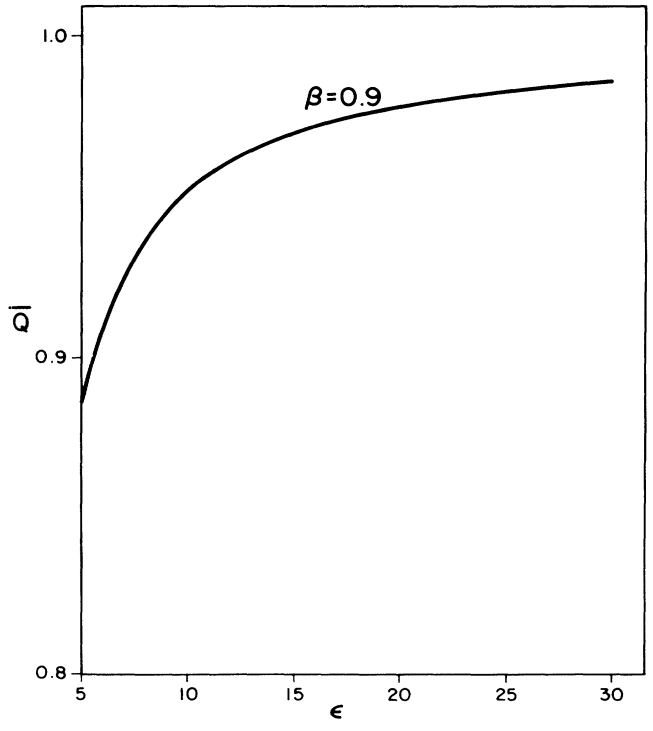

FIG. 8. The dependence of the geometric factor $\bar{Q}$ on the dielectric coefficient.

where $\eta=k_e h/\gamma$ measures the height of the beam, $\delta=k_e\Delta/\gamma$ gauges its thickness, and $\tau=[1-(\omega_p/V_0/\gamma)^2/q^2]^{1/2}$. This is our equation for q, the change of the propagation constant due to the beam-wave interaction. The positive imaginary part of the solution for q gives the gain per unit length, and the real part indicates the change of the phase velocity of the synchronous wave. Equation (3.15) can be cast into a dimensionless equation for $\bar{q}=q/k_e$, i.e.,

$$\bar{q}^3=-\frac{\Omega^2}{\gamma^2}\frac{e^{-2\eta}\sinh(\tau\delta)}{\tau\cosh(\tau\delta)+\frac{1}{2}(1+\tau^2)\sinh(\tau\delta)}\bar{Q}\ , \tag{3.16}$$

where $\Omega=\omega_p/(\omega\gamma)$ is usually very small. This equation can now be solved numerically for different parameters of the beam.

In the strong-coupling regime $|q|$ the deviation from synchronization is much larger than the plasma wave vector ω_p/c, but still much smaller than the radiation wavelength or grating periodicity. In this case τ may be replaced by 1 and Eq. (3.16) yields

$$\bar{q}^3=-\frac{\Omega^2}{\gamma^2}e^{-2\eta}e^{-\delta}\sinh(\delta)\bar{Q}\ . \tag{3.17}$$

[For the opposite case, i.e., $|q|\ll\omega_p/c$, Eq. (3.16) reads $\bar{q}^3=2\bar{q}^2\bar{Q}e^{-2\eta}/\gamma^2$ and its solutions are $\bar{q}_1,\bar{q}_2=0$ and $\bar{q}_3=\bar{Q}e^{-2\eta}/\gamma^2$; these solutions do not correspond to an energy exchange process and no gain occurs.]

Since we are interested here in the SPA operation in the exponential gain regime, we confine our analysis hereafter to Eq. (3.17). Notice that this equation holds even for a slender beam, when the current ($\propto\omega_p^2\Delta$) is finite. The right-hand side of Eq. (3.17) is thus a negative real number, and this cubic equation for $\bar{q}$ is similar to Pierce's traveling-wave solution. We now return to the original variables, define

$$\tilde{q}=\left[\left[\frac{\omega_p}{c}\right]^2\frac{\omega}{c}\frac{1}{\gamma^4}\left[\frac{c}{V_0}\right]^3 e^{-2\eta}e^{-\delta}\sinh(\delta)\bar{Q}\right]^{1/3} \tag{3.18}$$

and write Eq. (3.17) as $q^3=-\tilde{q}^3$. This equation has three solutions: one is real, $q_1=-\tilde{q}$, and the other two are complex, i.e., $q_2=\tilde{q}e^{j5\pi/3}$ and $q_3=\tilde{q}e^{j\pi/3}$. The last solution, q_3, corresponds to a growing wave, which propagates with a phase velocity somewhat smaller than the beam velocity. Similar solutions were found in the context of the free-electron laser by Kroll[23] and recently were also studied by us.[24,25]

We can now estimate the exponential gain of the Smith-Purcell amplifier, i.e., the imaginary part of q_3. From Eq. (3.18) we see that the gain can be expressed in terms of the current of the beam ($I\propto\omega_p^2\Delta$) or in terms of its density n_0. In Fig. 9 we show the normalized gain as a function of the beam thickness. Curve (1) depicts the gain when the current is held constant. The normalized gain is then written as $g/g_I=[e^{-\delta}\sinh(\delta)/\delta]^{1/3}$ where

$$g_I\equiv\frac{\sqrt{3}}{2}\left[\frac{I\eta_0}{mc^2/e}\frac{\left[\frac{\omega}{c}\right]^2}{\Delta_y}\frac{l^{-2\eta}}{\gamma^6\beta^5}\right]^{1/3}$$

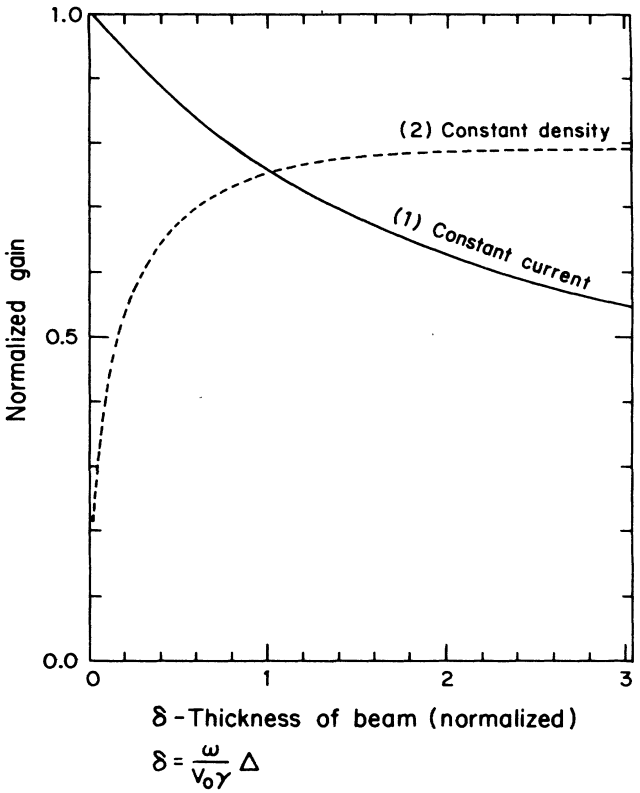

FIG. 9. The dependence of the gain on the thickness parameter of the beam for a constant current and a constant density.

is the normalization factor for constant current. This gain has a maximum for a slender beam ($\delta\to0$) and gets weaker for thicker beams. We can understand this result considering that the beam-wave coupling is weaker for the distant electrons. Curve (2) is the corresponding gain, $g/g_n=[e^{-\delta}\sinh(\delta)]^{1/3}$, when the beam density is held constant and

$$g_n\equiv\frac{\sqrt{3}}{2}\left[n_0\frac{e\eta_0\omega}{mc^2/e}\frac{e^{-2\eta}}{\gamma^5\beta^3}\right]^{1/3}.$$

To get a feeling for the order of magnitude of the gain we take $V_0/c=0.9$, $\lambda=10^{-3}$ m, $h=0.5\times10^{-3}$ m. If we assume that the current is 1 A (and the width of the beam in the y direction is 0.1 m) we find $g_I=5.22\ \mathrm{m}^{-1}$. For a density of $n_0=2\times10^{14}\ \mathrm{m}^{-3}$ we have $g_n=60\ \mathrm{m}^{-1}$.

The dependence of this exponential gain on the beam height h above the grating has a simpler form and it decreases exponentially as $\exp[-\frac{2}{3}(\omega/V_0\gamma)h]$. This result is not applicable for distant beams, since the strong-coupling condition $|\bar{q}|<\omega_p/c$ does not hold any more, but then Eq. (3.16) can be solved numerically.

IV. THE OSCILLATOR

A. General

In Sec. III we have found that injecting a beam of electrons above a corrugated surface, which is externally il-

luminated, may cause extraction of kinetic energy from the beam. This extraction process increases *exponentially* with the length of the interaction domain. In the present section we suggest the construction of an oscillator whose startup is provided by the Smith-Purcell radiation and its steady-state oscillations are sustained by this amplification process. A similar oscillator was proposed by Wachtel[5]—see Fig. 10(a)—but his analysis was based on the assumption that the extraction rate increases *algebraically* with the interaction length—or to be more specific, the resulting gain is proportional to the third power of this length. We expect the extraction rate in our case to be much larger, the device to be more efficient, and the necessary current (threshold) to sustain the oscillation to be lower.

B. Design principles

The Smith-Purcell oscillator is composed of three parts: (i) an active component (grating plus beam), (ii) electromagnetic waves, and (iii) a feedback system (see Fig. 10). The first component characteristics are identical with those introduced in Secs. II and III, namely, a grating of a periodicity L, whose unit cell is of a given geometry, and a beam of electrons at a height h above the surface, with average velocity V_0, beam density n_0, and thickness Δ. According to the Smith-Purcell effect (Sec. II B 3), a beam of electrons which moves above a grating emits radiation. In the SPO, part of this radiation is "captured" by the feedback system and is reflected back towards the grating. This incident wave, in turn, is scattered by the grating and it is slightly amplified by the beam, which now "operates" as an active medium. This process keeps repeating itself and the total electromagnetic wave is a superposition of all these contributions. From this brief description we expect that the frequency of the EM wave is mainly determined by the SP radiation, since it provides the "startup" to the entire process. In Sec. II B 3 we discussed the characteristics of SP radiation and we observed there that in a given direction, say, an angle θ with the z axis (see Fig. 11), a detector would have measured certain frequencies, which up to an integer P are determined in terms of the grating periodicity (L), electron velocity (V_0), and the detector angle (θ), namely,

$$\omega_0=\frac{2\pi}{L}c\frac{1}{1/\beta-\sin\theta}P \ . \tag{4.1}$$

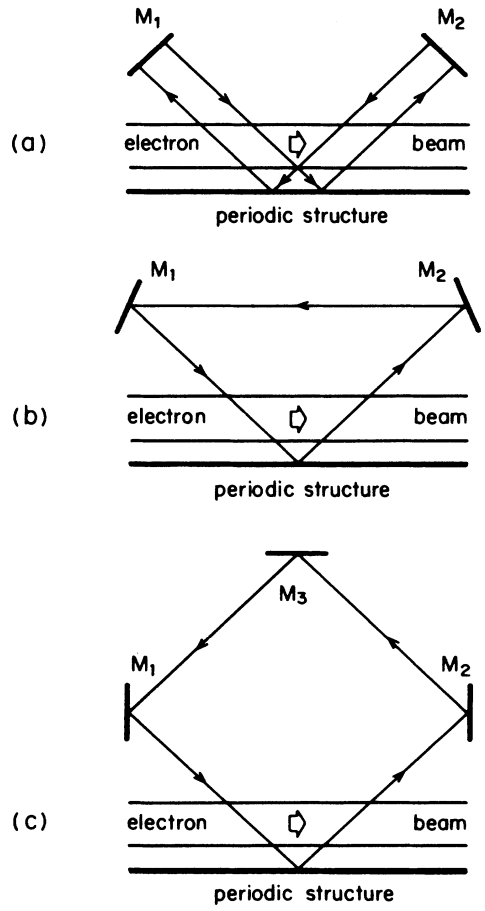

FIG. 10. (a) is the Smith-Purcell oscillator as proposed by Wachtel. (b) and (c) are two possible configurations for a high-frequency oscillator.

In the oscillator mode of operation the detector is "replaced" by a feedback system made of three mirrors. In the present section we wish to determine the relative position of these mirrors in order to support the oscillations. Since we wish our oscillator to operate near the SP frequency ω_0 (for given β and L), the mirror M_2 has to be located so that it would "collect" the wave which leaves the grating with an angle θ—see Fig. 11. Obviously, many other waves may hit this mirror, however, we intend to arrange the other two mirrors in a manner such that only a *single feedback wave* (SFW) completes the feedback loop. Actually there is a large number of possible setups which fulfill this condition, however, their number is significantly reduced when stability is required.

Let us assume for the moment that these mirrors are located so that only the wave with a frequency ω_0 propagates in the feedback system. This SP frequency of the spontaneous emission was calculated assuming that the electron's velocity is constant and uniform. However, at the presence of the induced EM field the electronic motion is perturbed (rippled), and in turn a small deviation from the "initial" frequency occurs. This deviation can cause an angular deflection of the FW, and as a result the latter would "escape" from the oscillator. To avoid this, we require the system to be stable under small deviations from the SP frequency. Adopting the Floquet notation, the x component of the feedback wave vector, which leaves the grating with an angle $\psi_{\text{out}}(=\theta)$, is given by

$$\frac{\omega_0}{c}\sin\psi_{\text{out}}=k_{\text{out}}+\frac{2\pi}{L}n_{\text{out}} \ , \tag{4.2}$$

and the incident feedback wave vector, which impinges on the grating with an angle ψ_{in}, is

$$\frac{\omega_0}{c}\sin\psi_{\text{in}}=k_{\text{in}}+\frac{2\pi}{L}n_{\text{in}} \ . \tag{4.3}$$

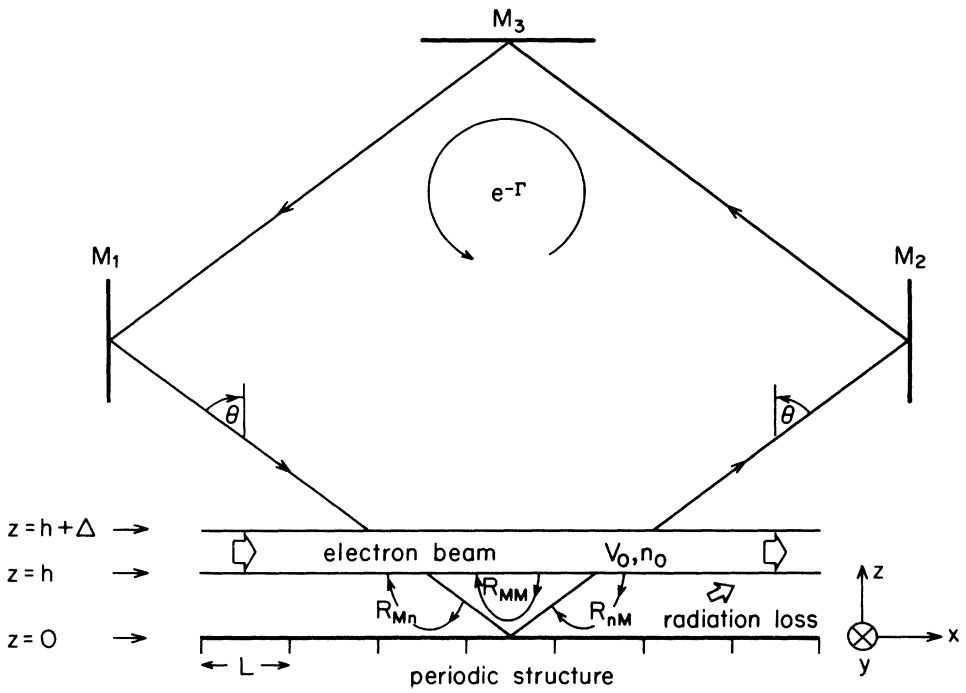

FIG. 11. Smith-Purcell oscillator. The mirror M_2 collects waves of different frequencies (as determined by Smith-Purcell relation) but only those leaving the grating with an angle θ are returned to the active region by the feedback system. The role of the different terms (R_{Mn}, R_{MM}, and R_{nM}) of the oscillator dispersion relation is illustrated.

Since the grating couples only between Floquet harmonics with the same wave vector in the first Brillouin zone, we conclude that $k_{\text{in}}=k_{\text{out}}\equiv k_0$, and subtracting Eq. (4.3) from Eq. (4.2) we find

$$\sin\psi_{\text{out}}=\sin\psi_{\text{in}}+\frac{2\pi}{(\omega_0/c)L}(n_{\text{out}}-n_{\text{in}}) . \tag{4.4}$$

The effect of the electronic ripples is expressed by the small changes $\delta\omega$ and δk in the frequency and the wave vector, respectively, i.e., ω_0 is replaced by $\omega=\omega_0+\delta\omega$ and k_0 by $k=k_0+\delta k$. We wish to emphasize that this deviation is so small that it does not affect the harmonics indexes. The "new" waves propagate within two directions determined by

$$\sin\psi'_{\text{out}}=\frac{\left[k_0+\delta k+\frac{2\pi}{L}n_{\text{out}}\right]}{\left[\frac{\omega_0+\delta\omega}{c}\right]}$$

$$\sim\sin\psi_{\text{out}}\left[1+\frac{\delta k}{k_0+(2\pi/L)n_{\text{out}}}-\frac{\delta\omega}{\omega_0}\right] \tag{4.5}$$

and

$$\sin\psi'_{\text{in}}=\frac{\left[k_0+\delta k+\frac{2\pi}{L}n_{\text{in}}\right]}{\left[\frac{\omega_0+\delta\omega}{c}\right]}$$

$$\sim\sin\psi_{in}\left[1+\frac{\delta k}{k_0+(2\pi/L)n_{\text{in}}}-\frac{\delta\omega}{\omega_0}\right] . \tag{4.6}$$

The stability condition implies that these "new" angles are identical with the initial ones within the approximation of small $|\delta k|$ and $|\delta k|$ (i.e., $|\delta\omega|\ll\omega_0$ and $|\delta k|\ll|k_0|$). As a consequence of this condition we find that the last term of Eqs. (4.5) and (4.6) has to vanish, i.e.,

$$\frac{\delta k}{k_0+(2\pi/L)n_{\text{out}}}-\frac{\delta\omega}{\omega_0}=0 \tag{4.7}$$

and

$$\frac{\delta k}{k_0+(2\pi/L)n_{\text{in}}}-\frac{\delta\omega}{\omega_0}=0 , \tag{4.8}$$

which in turn imply that $n_{\text{out}}=n_{\text{in}}\equiv n$, and finally that

$$\psi_{\text{out}}=\psi_{\text{in}}=\theta . \tag{4.9}$$

In other words, the mirror M_1, see Fig. 11, should be placed in such a way that the reflected FW imginges on the grating with the same angle as it leaves it.

The simplest realization of the stability condition is a two-mirror system, say M_1 and M_2 positioned so that the FW is reflected by M_2 directly towards M_1 [see Fig. 10(b)]. Let us, in this simple case, follow after a single ray. Starting from a point on the grating and completing an entire loop, it can be readily seen that we do not return to the starting point; this point can be reached only after completing an additional loop. Obviously at each point there are *two* waves with the same ω and k but with different phases, and thus a destructive interference between these waves might occur. In order to avoid this situation, we have introduced an additional mirror M_3 [see Fig. 10(c)]. Now that the relative position of the mir-

rors is known, their position will be expressed in terms of the optical length d_{opt} the FW has to travel to complete an entire loop. This is described, together with the condition for oscillations to be sustained, in Sec. IV C. Nevertheless, two "crude" bounds of this length scale can now be estimated: the mirrors have to be relatively *close* to each other, enough that *diffraction* effects can be neglected; this condition provides an upper bound to d_{opt}. The lower bound can be estimated by requiring that M_1 and M_2 have to be far away from the beam and the grating, so that their influence on the beam-wave interaction is negligible.

C. The condition for self-sustained oscillations

Consider a device which fulfills all the conditions mentioned in Sec. IV B. Our purpose in this section is to determine the necessary conditions for oscillations to be sustained in our device. Since the grating and the feedback system are given, our "degree of freedom" is the beam, and therefore this condition will be formulated in terms of the minimal necessary current that sustains EM oscillation of frequency near ω_0.

Since the feedback mirrors are of finite sizes, the EM field which propagates in the feedback loop is confined to a limited beamlike domain—EM beam. Neglecting diffraction effects, we assume that the EM field in this domain can be described by a plane wave. The incident wave, oscillating at a frequency ω, and propagating from the mirror M_1 towards the grating, is written as

$$H_y^{(in)}(x,z,t)=F_n(\omega,k)\exp(j\omega t-jk_n x+\beta_n z) . \tag{4.10}$$

We have previously shown [Eq. (3.7)] that when a plane wave hits the system of a grating and a beam (which moves above the grating), the amplitude D_n, of the wave

$$H_y^{(ref)}(x,z,t)=D_n(\omega,k)\exp(j\omega t-jk_n x-\beta_n z)$$

which is reflected towards the mirror M_2, is given by

$$D_n=\left[R_{nn}+R_{nM}\frac{1}{1/U_M-R_{MM}}R_{Mn}\right]F_n . \tag{4.11}$$

The feedback system, of optical length d_{opt}, returns this wave back towards the grating with its phase shifted by an amount $\exp[-j(\omega/c)d_{opt}]$—see Fig. 11. Mirror losses and energy extraction from the oscillator may decrease the field amplitude. These losses are denoted by r. It is convenient now to define the total reflection coefficient of the feedback system as $\exp(-\Gamma)=r\exp[-j(\omega/c)d_{opt}]$ where Γ is a complex quantity. The amplitude of the FW, when it returns to the active region, is $D_n\exp(-\Gamma)$. Since we have started with the wave of Eq. (4.10), the SWF assumption dictates that $D_n\exp(-\Gamma)=F_n$, and thus with Eq. (4.11) we have

$$\left[R_{nn}+R_{nM}\frac{1}{1/U_M-R_{MM}}R_{Mn}\right]e^{-\Gamma}\equiv 1 . \tag{4.12}$$

Equation (4.12) is our result for the dispersion relation in a Smith-Purcell oscillator. For the given system's parameters, i.e., the electron beam, the grating, and the "circuit," one should solve Eq. (4.12) for the operating frequency ω of the oscillator. The wave vector in the first Brillouin zone k is expressed in this equation in terms of the constraint imposed by the feedback system, namely, only a wave leaving the grating within an angle θ completes the loop. This constraint is mathematically formulated as follows:

$$k=\frac{\omega}{c}\sin\theta-\frac{2\pi}{L}n . \tag{4.13}$$

We wish to point out that though the frequency, as appears in Eqs. (4.10), (4.11), and (4.13) is real, the dispersion equation is understood as an analytical continuation of Eq. (4.12) into the ω complex plane. The complex frequency $\omega=\omega_r+j\omega_i$ that solves this equation gives the operating frequency ω_r of the oscillator, and if ω_i is negative, kinetic energy of the beam is turned into net radiation energy, which can be extracted from the system. However, we should notice that this procedure would yield reasonable results only if ω_i is very much smaller than ω_r. We should further observe that since the driving mechanism for starting the self-sustained oscillations is the Smith-Purcell spontaneous radiation, we expect the operating frequency ω to be close to ω_0 of Eq. (4.1). This change of frequency is understood as due to the perturbation of the electronic motion by the EM field.

An additional insight into Eq. (4.12) can be obtained by reorganizing its terms in a different way, namely,

$$\frac{1}{U_M}-R_{MM}=\bar{R}_{MM} , \tag{4.14}$$

where

$$\bar{R}_{MM}\equiv R_{Mn}R_{nM}e^{-\Gamma}/(1-R_{nn}e^{-\Gamma}) .$$

The left-hand side of this equation is recognized from the SP amplifier [Eq. (3.10)], and is related to the positive gain, i.e., to extraction of kinetic energy from the beam. The right-hand side, $\bar{R}_{MM}$, describes the feedback, and it contains two different loss mechanisms which will be discussed later.

Before we proceed we shall determine the harmonics indexes M and n in Eq. (4.12). Actually what we know is that the SP frequency is determined in Eq. (4.1), up to an integer P. Eliminating k_0 from $\omega_0/V_0=k_0+2\pi M/L$ and $(\omega_0/c)\sin\theta=k_0+2\pi n/L$ we find that $P=M-n$. If we confine our analysis to the lowest possible frequency, i.e., $P=1$, then k_0 and M are determined by the requirement that k_0 itself should be in the first Brillouin zone, i.e.,

$$-\frac{\pi}{L}<k_0=\frac{2\pi}{L}\frac{M\beta\sin\theta-n}{1-\beta\sin\theta}<\frac{\pi}{L}\quad\left[\beta=\frac{V_0}{c}\right] ,$$

and by taking $n=M-1$. The $P=1$ choice is justified by the fact that Smith-Purcell radiation decays exponentially away from the grating with an exponent whose argument is proportional to the frequency (and to the height of the beam)—as shown in Sec. II B 3.

In order to solve Eq. (4.12) for a particular SP oscillator we have to calculate the relevant elements of the

reflection matrix for a given grating. Actually, we must determine only the four elements R_{MM}, R_{nM}, R_{Mn}, and R_{nn} near the SP frequency ω_0. However, we wish to emphasize that if the condition for the existence of oscillations is not fulfilled, then the alternative solution is $F_n=D_n=0$, which obviously implies that no self-sustained EM field exists. The transition between these two regimes is controlled by the current intensity. This quantity decides whether the sign of the imaginary part of the frequency which solves Eq. (4.12) is positive or negative. It is the negative imaginary part which corresponds to a growing solution.

D. The threshold current

The current which determines the transition between these two regimes is called the threshold current ($I_{\rm th}$). If we could solve exactly Eq. (4.12), then this current could be determined from the condition

$$\omega_i=0 \ . \tag{4.15}$$

Exact solution of Eq. (4.12) can be rather difficult, and we intend here to provide only an approximate calculation of this current. For this purpose we adopt a different procedure, which is quite common when studying oscillators; we assume that the imaginary part of the frequency consists of two terms

$$\omega_i=\omega_i^-+\omega_i^+ \ . \tag{4.16}$$

The first term (ω_i^-) results from the different loss mechanisms and it *always* causes a decrease of the field amplitude. The second term (ω_i^+) is due to the extraction of kinetic energy from the beam, and it may cause an *increase* in the field amplitude. In our approximate procedure we calculate each of these quantities ignoring the competing mechanism; in other words, we calculate ω_i^+ assuming that there are no losses (i.e., $\omega_i^-=0$) and ω_i^- is established by leaving out the extraction mechanism (i.e., $\omega_i^+=0$). A partial support to this procedure is provided by Eq. (4.14), where we identified the left-hand side ($1/U_m-R_{MM}$) as associated with the energy extraction, and the right-hand side, $\bar{R}_{MM}$, with the loss mechanisms.

Evaluation of ω_i^+ is accomplished much in the spirit of Sec. III B, namely, we solve

$$\frac{1}{U_M}-R_{MM}=0 \tag{4.17}$$

for ω_i^+. If the grating supports the synchronous wave M then R_{MM} can be approximated near the SP frequency ω_0, by

$$R_{MM}=-\frac{2\omega_0/\beta\gamma^2}{\Omega}\tilde{Q} \ , \tag{4.18}$$

where $\Omega=\omega-\omega_0$ and $\tilde{Q}$ depends on the geometry, is real, and of order of 1. In the strong-coupling regime ($\omega_p \ll |\Omega|$) we write U_M as

$$U_M=-\frac{e^{-2\eta}}{2}\frac{\omega_p^2}{\gamma^2\Omega^2(1-\beta\sin\theta)^2}e^{-\delta}\sinh(\delta) \ , \tag{4.19}$$

where $\eta=(\omega_0/V_0\gamma)h$ and $\delta=(\omega_0/V_0\gamma)\Delta$. Using Eqs. (4.18) and (4.19) we turn Eq. (4.17) into a cubic equation for Ω, i.e., $\Omega^3=\Omega_0^3$ where $\Omega_0=\omega_0(I/I_0)^{1/3}$, $I=en_0V_0\Delta\Delta_y$ is the current injected in our system,

$$I_0=\frac{mc^2}{e\eta_0}\frac{(\gamma^2\beta)^3(1-\beta\sin\theta)^2[(\omega_0/c)\Delta_y]}{\tilde{Q}[e^{-2\eta}e^{-\delta}(\sinh\delta)/\delta]} \ ,$$

and $\eta_0=(\mu_0/\epsilon_0)^{1/2}$ is the vacuum characteristic impedance. This cubic equation is the analog to that obtained in the preceding section for the wave vector of the SW in the SPA. We are interested here in conversion of beam energy into radiation energy, and thus consider only the growing wave solution with positive growth rate $\omega_i^+=-\sqrt{3}/2\Omega_0$. We wish to emphasize that this gain coefficient is common to *all* the waves including our FW, since the boundary conditions at the grating must be satisfied at any instant.

Disregarding the beam, we now turn to evaluate the losses, in a way similar to the calculation of the quality factor of a cavity in microwave devices. There are here three different loss mechanisms: (a) radiation losses by scattering at the periodic surface, (b) losses due to the finite conductivity of the metallic surfaces (like mirrors and grating), and (c) radiation losses due to extraction of energy through one of the mirrors. As we shall consider only the threshold conditions for the oscillator operation, it will be assumed that no energy is extracted out of the oscillator. First we determine the power lost by the scattered radiation at the grating. We assume that an incident radiation beam of cross section A impinges on the grating; the amplitude of the magnetic field is H_0, and the incident power is $P^{(\rm inc)}=\eta_0(|H_0|^2/2)A$. The useful power which is reflected towards the feedback trajectory (M_2) is approximately given by $P^{(\rm sc)}=P^{(\rm inc)}|R_{nn}|^2$, and thus the radiation losses (subscript r) are given by

$$P_{r,\rm loss}=P^{(\rm inc)}-P^{(\rm sc)}=\eta_0\frac{|H_0|^2}{2}A(1-|R_{nn}|^2) \ . \tag{4.20}$$

The power loss due to finite conductivity of, say, mirror M_1, which has an angle $\pi/2-\theta$ with respect to the radiation beam is

$$P_{m,\rm loss}=\eta_0\frac{|H_0|^2}{2}A\left[4\left[\frac{\omega_0\epsilon_0}{\sigma}\right]^{1/2}\frac{1}{\sin\theta}\right] \ ,$$

where σ is the conductivity. Similar expressions for the finite conductivity losses of the other mirrors and the grating are expected to be of the same order of magnitude. Let us now compare these two loss mechanisms. Both the mirrors and the grating are made of a high-conductivity material, say, $\sigma\sim10^7$ mho/m, thus for millimeter waves—at which we expect our device to operate—the term in square brackets of $P_{m,\rm loss}$ is of the order of 10^{-3} (taking $\sin\theta\sim1$). On the other hand, for wavelengths λ smaller than L the term in square brackets in Eq. (4.20) is of the order unity, and thus we conclude that in our regime of operation the principal loss mechanism is due to radiation scattering. Since the total energy stored in the entire oscillator is given by $W_{em}=\mu_0(|H_0|^2/2)Ad_{\rm opt}$, the decay rate in the small loss

regime, is estimated as

$$2/\tau_{\rm loss}=P_{r,\rm loss}/W_{em}=(c/d_{\rm opt})(1-|R_{nn}|^2)\ .$$

The necessary condition for oscillations to sustain is that this decay rate will be smaller or equal to the growth rate calculated above, i.e.,

$$\omega_i^+=\frac{\sqrt{3}}{2}\omega_0\left[\frac{I}{I_0}\right]^{1/3}\geq\omega_i^-=\frac{c}{2d_{\rm opt}}(1-|R_{nn}|^2)\ . \quad (4.21)$$

This, in turn, gives us the threshold current in terms of the other parameters of the system, namely,

$$I_{\rm th}=0.192I_0\left[\frac{1-|R_{nn}|^2}{(\omega_0/c)d_{\rm opt}}\right]^3\ . \quad (4.22)$$

This is the main result for the threshold current of our SP oscillator.

To estimate numerically the threshold current we consider now an instructive example, a periodic structure composed of a smooth surface where half of the unit cell $(0<x<L/2)$ is made of a high conductive material $(\sigma\rightarrow\infty)$, and the other half $(L/2<x<L)$ is made of a high magnetic permeability material $(\mu_r\rightarrow\infty)$. Taking $\theta=75°$ and $\lambda=10^{-3}$ m we find that $n=4$, and the corresponding term of the reflection matrix R_{44} is $-0.54+0.35j$. For the following characteristic parameters: $\Delta=10^{-3}$ m, $|\bar{Q}|=1$, $h=0.5\times10^{-3}$ m, $\Delta_y=0.1$ m, $d_{\rm opt}=0.2$ m, and $\beta=0.9$ we find that this current is $I_{\rm th}=3.8\times10^{-3}$ A.

This result for the threshold current should be compared with that obtained by using Wachtel's[5] suggestion for a similar SP oscillator. First we estimate the power transferred by the electrons to the radiation in the presence of an *almost* synchronous wave. Notice that the operating regime is different from the one considered by us, that is, the electrons act as an ensemble of synchronized "antennas" and the slow wave is *assumed* to remain *unchanged,* while in our case the slow wave does change along the interaction domain, and is solved in a *self-consistent* manner. This domain in Wachtel's oscillator is approximately $2D\sim A/\Delta_y\cos\theta$, and thus the power exchanged is given by

$$P=\omega_0 W_{em}\frac{I}{I_0}\left[\frac{2D}{d_{\rm opt}}\right]\left[\frac{\omega_0}{c}2D\right]\left[\frac{\gamma}{\beta^2}\frac{(1-\beta\sin\theta)^2}{Q\cos\theta}\right]$$
$$\times|R_{Mn}|^2\left[-\frac{1}{2}\frac{d}{d\xi}\mathrm{sinc}^2(\xi)\right]\ ,$$

where

$$\xi=\left[\frac{\omega_0}{V_0}-\frac{\omega_0}{c}\sin\theta-\frac{2\pi(M-n)}{L}\right]D\ .$$

Only a part, $|R_{nM}|^2$, of this power is transferred to the FW. Following a similar procedure as previously and considering the maximum gain $(\xi=-1.3)$ obtained for $2D\sim0.1$ m, we find that the threshold current is given by

$$I_{\rm th}=I_0\frac{(1-|R_{nn}|^2)}{|R_{nM}R_{Mn}|^2}\frac{\beta^2\cos\theta}{0.27\gamma(1-\beta\sin\theta)^2[(\omega_0/c)2D]^2}\ . \quad (4.23)$$

In Wachtel's case, the system does not operate as close to resonance as in ours, and therefore we expect the matrix elements to behave rather regularly. We assume $|R_{Mn}|$ and $|R_{nM}|$ to be of order unity and find for a very thin beam $(\delta\rightarrow0)$, which almost touches the grating $(\eta\rightarrow0)$—these are Wachtel's assumptions—that the threshold current is $I_{\rm th}\sim38$ A. This current is much larger than that found in our scheme, since the energy extraction rate from the electrons is much smaller. The difference is even more significant if we take into account the beam thickness and its height above the grating. In that case, for the previous parameters, the threshold current is $I_{\rm th}\sim0.56$ kA.

V. DISCUSSION

In the present study we investigated the energy exchange between electrons and electromagnetic waves in the presence of a periodic structure. This process had been examined extensively in the past mainly in *closed* periodic structures, namely, slow waveguides. Here we concentrate on the interaction of an electron beam with electromagnetic waves in an *open* periodic structure, i.e., in a Smith-Purcell system. This will open up the way to tunable radiation sources of shorter wavelengths, from millimeter waves to soft x rays. The main disadvantage of a periodic waveguide is the multitude of modes, which are excited if the cross section of the system is not small. In order to retain a small number of modes the cross-section dimensions should be of the order of the operating wavelength and waveguides with dimensions less than 1 mm are hard to come by.

Let us now summarize the main conclusions of the present study of the Smith-Purcell free-electron laser, in the exponential gain regime.

(a) When operated as an amplifier, it is shown that exponential gain can be developed in this device, namely, the amplitude of the electromagnetic field increases exponentially along the interaction region.

(b) The influence of the beam height h on the gain is shown to be considerable since it decreases exponentially with the height, i.e., the gain $\propto\exp(-2/3(\omega/\gamma V_0)h]$.

(c) The effect of the thickness of the beam on the gain is also considered here. We find that when operating at *constant current,* the gain decreases algebraically with the beam thickness Δ, i.e., the gain $\propto\Delta^{-1/3}$. When operating at *constant density* the gain increases with the thickness, up to an asymptotic value which is reached when $\omega\Delta/\gamma V_0\sim2$.

(d) It is suggested to utilize the energy extracted from the beam to construct an oscillator. The threshold current is determined and it is found to be much smaller than that necessary for a device operating in the algebraic gain regime.

In the course of our analysis, it was assumed that an *ideal* beam is injected into the system. This means that the longitudinal momentum distribution is extemely peaked (Dirac δ function) and the transversal electron motion vanishes. In practice the momentum distribution is of a finite width; we denote the longitidinal velocity spread by V_L, and the transversal one by V_T. Let us now

estimate the bounds on these two parameters for our analysis to remain reasonable. (a) The transversal spread V_T has no contibution to the interaction, and it should be limited by the condition that the electrons do not hit the grating because of their transversal motion. To calculate this limit, we consider an electron moving with a velocity V_0 parallel to a grating of length D at a height h above it; the time it takes the particle to cross the device is approximately D/V_0. If its initial transverse motion (towards the grating) is V_T then the electron would not hit the surface if

$$\frac{V_T}{V_0} < \frac{h}{D} . \tag{5.1}$$

(b) To determine the upper bound for the longitudinal spread, we adopt Kroll's[23] approach, originally applied to a bremsstrahlung FEL. As in the magnetic wiggler case, the current is determined by integration over the product of a peaked distribution function and a resonance term of the $1/(\omega - Vk_M)$, where ω is the radiation frequency, V is the electron velocity, and k_M is the synchronous wave number. Notice that k_M may have a small imaginary part. Our analysis will remain accurate when the longitudinal spread V_L is much smaller than the width of the resonance term, $(\omega/|k_M|^2)\mathrm{Im}(k_M)$, or

$$\frac{V_L}{V_0} < \frac{\mathrm{Im}(k_M)}{|k_M|} . \tag{5.2}$$

It is more convenient to express the beam quality in terms of the energy spread $\Delta\gamma$ which is related to V_L through $\Delta\gamma/\gamma = (V_L/V_0)(\gamma\beta)^2$; substituting the explicit expression for $\mathrm{Im}(k_M)$ and normalizing the current I so that $\bar{I} = Ie(\mu_0/\epsilon_0)^{1/2}/mc^2$ we obtain

$$\frac{\Delta\gamma}{\gamma} < \frac{\sqrt{3}}{2}\beta \left[\bar{I} \frac{1}{(\omega/V_0)\Delta_y} e^{-2\eta} e^{-\delta} \frac{\sinh(\delta)}{\delta} \right]^{1/3} ,$$

$$\eta \equiv \frac{\omega h}{\gamma V_0}, \quad \delta \equiv \frac{\omega \Delta}{\gamma V_0} . \tag{5.3}$$

For our previous numerical example $\lambda = 10^{-3}$ m, $\Delta = 10^{-3}$ m, $\beta = 0.9$, $h = 0.5 \times 10^{-3}$ m, $\Delta_y = 0.1$ m, and $I = 0.5$ A we find that $\Delta\gamma/\gamma < 1.2 \times 10^{-3}$, which is a reasonable spread. Also for a device of length $D = 0.3$ m, the transversal spread is of the same order of magnitude, i.e., $V_T/V_0 < 1.67 \times 10^{-3}$. These estimates suggest that for millimeter wavelengths the conditions on the beam quality are not too stringent.

A tunable source of radiation is of importance also for wavelengths shorter than millimeter wave. The major problem then is the fact that the beam height above the grating has to be of the same order of magnitude as the radiation wavelength, otherwise the exponential decay "kills off" the interaction. It is not easy to inject an electron beam of a significant current as close as one micron to the grating. Another obstacle is the electromagnetic and geometric properties of the grating at these higher

TABLE III. The limiting value of the beam spread $\Delta\gamma/\gamma$ for different wavelengths. We consider here a grating of 10 μm periodicity, a beam of 0.5 μm thickness, 0.5 μm width injected at a height 0.5 μm above the grating. The radiation which propagates parallel to the beam, $\theta = \pi/2$, consists of many frequencies determined by n. Only the first two, $n = -1$ and -2, are considered. The first two columns determine the γ necessary to obtain the corresponding wavelength λ in the same row. In the last two columns we calculate the maximum value of the energy spread allowed in order that the exponential gain will occur. From this table we conclude that although the energy necessary to obtain the same wavelength is lower when working with $n = -2$, the beam quality has to be much higher comparing both with the case $n = -1$. In general, we shall prefer to work with higher energy (which is easier to obtain) and relatively low beam quality rather than the opposite case. $x[y] = x \times 10^y$.

	λ		$\frac{\Delta\gamma}{\gamma}\frac{1}{[I(\mathrm{A})]^{1/3}}$	
	$n=-1$	$n=-2$	$n=-1$	$n=-2$
Submillimeter				
$\lambda = 100$ μm	1.004	1.001	0.729[−2]	0.228[−2]
Far infrared				
$\lambda = 10$ μm	1.15	1.06	0.271[−1]	0.115[−1]
Infrared				
$\lambda = 1$ μm	2.40	1.81	0.125[−1]	0.651[−2]
Visible				
$\lambda = 0.5$ μm	3.28	2.40	0.654[−1]	0.307[−2]
Ultraviolet				
$\lambda = 0.1$ μm	7.12	5.07	0.611[−3]	0.155[−3]
XUV				
$\lambda = 0.05$ μm	10.04	7.12	0.128[−3]	0.198[−4]
X-ray				
$\lambda = 0.01$ μm	22.38	15.84	0.325[−6]	0.595[−8]

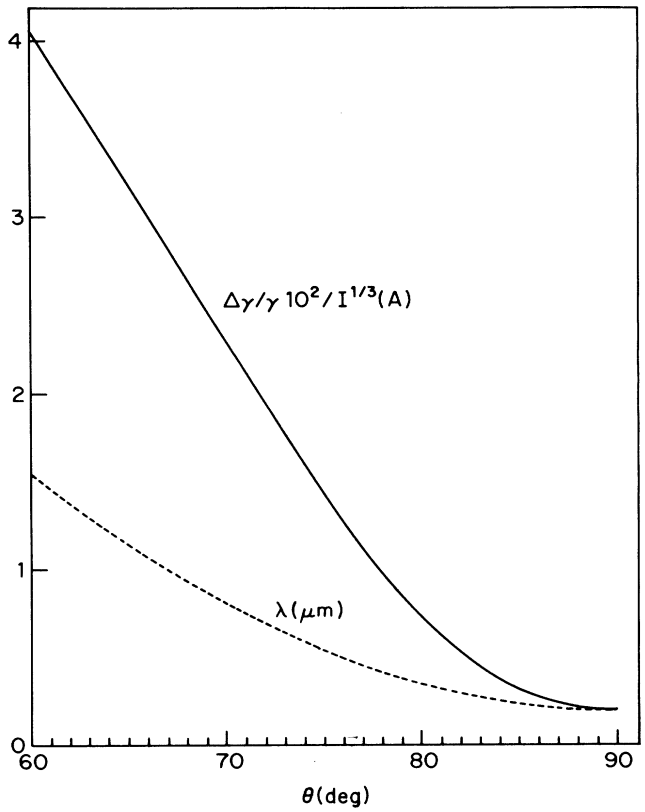

FIG. 12. The allowed energy spread vs the feedback angle θ. The radiation wavelength is also depicted. $\gamma=5$.

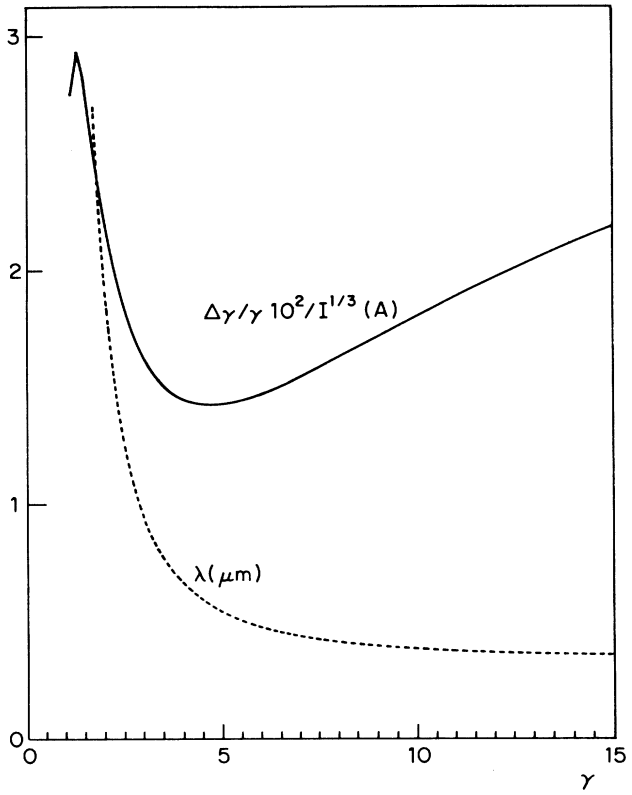

FIG. 13. The allowed energy spread vs the electron energy γ. The feedback angle is $\theta=75°$. The radiation wavelength is also depicted.

frequencies. Below 0.5 μm, for example, the conductivity of metals (except aluminum) is very poor and a significant part of the radiation will be absorbed by the grating or transferred through it. Moreover, there appear microirregularities in the fabrication process, whose characteristic length is of the same order of magnitude as the radiation wavelength, and it is hard to control their influence on the EM scattering processes. In spite of these problems let us determine, on the basis of our analysis, what are the necessary conditions on the beam parameters for operating the SP FEL in the wavelength domain below millimeter waves. In Table III we show the normalized longitudinal spread per current unit, $(\Delta\gamma/\gamma)(1/I^{1/3})(I$ in A), for a broad EM spectrum starting from submillimeter waves down to the soft x ray. These calculations were formed assuming that the grating periodicity is $L=10$ μm, the beam thickness, width, and height are $\Delta=0.5$ μm, $\Delta_y=0.5$ μm, and $h=0.5$ μm, respectively. In this table we consider only the first two waves, i.e. $n=-1,-2$ which propagate parallel to the beam, i.e., $\theta=\pi/2$. Comparing the first two columns we realize that it is preferable to use the "second wave" since the beam energy is lower. The opposite conclusion is reached when comparing the last two columns since the beam quality has to be much higher as dictated by the decrease in the allowed longitudinal spread. In general, it is much easier to obtain a beam with high γ rather than smaller spread $\Delta\gamma/\gamma$, therefore it will be preferable to utilize the "first wave."

In all these examples we have considered only waves which propagate parallel to the grating ($\theta=\pi/2$). One of the advantages of an open periodic structure is that we can utilize radiation which does not necessarily propagate parallel to the beam; to demonstrate this advantage let us consider the operation of this device as an oscillator. Two cases will be investigated: in the first the electron energy is kept constant and the angle of the feedback mirrors is changed; in the second the feedback remains unchanged and the electron energy is varied.

(i) An electron beam with $\gamma=5$ is injected above the grating (the beam and grating geometric properties are identical with the previous example). The mirrors are placed so that only radiation which leaves the grating with an angle θ (relative to the z axis) will be finally reflected back. Changing θ and keeping γ constant, different frequencies (for $n=-1$) can be obtained. In Fig. 12 the radiation wavelength is plotted versus the angle θ as well as the maximum longitudinal spread of energy per unit current. It is readily seen that as θ increases the Doppler shift is more accentuated, i.e., λ decreases, and also the beam quality increases.

(ii) In the second case the angle θ is kept constant and the γ of the electrons varies. Notice that for given θ and n there is a minimal wavelength $\lambda_{\min}$ due to the fact that the particle's velocity is always smaller than c, i.e.,

$$\lambda=L(1/\beta-\sin\theta)>L(1-\sin\theta)\equiv\lambda_{\min}\ .$$

All the wavelengths larger than $\lambda_{\min}$ can be obtained by

injecting a beam with a suitable energy. This is demonstrated in Fig. 13 where λ and the maximum allowed spread are plotted versus γ. Notice that while the wavelength decreases monotonically when γ increases, the relative spread, $\Delta\gamma/\gamma$, does not change monotonically as in the previous case. Around $\gamma \sim 4.78$ a very high-quality beam is necessary to obtain exponential gain. For γ larger than this value the necessary beam quality decreases monotonically. In all these cases, the transversal spread for a 1-cm-long device is $V_T/V_0 < 0.5 \times 10^{-4}$.

ACKNOWLEDGMENTS

This work is partially based on the D.Sc. thesis submitted to the Senate of the Technion by L.S. One of us (A.R.) wishes to acknowledge the support of the Fund for the Encouragement of Research at Technion. This research was supported by the Foundation for Research in Electronics, Computers and Communications, administered by the Israel Academy of Science and Humanities. We wish to thank Dr. N. Rostocker for useful discussion.

[1]S. J. Smith and E. M. Purcell, Phys. Rev. **92**, 1069 (1953).
[2]G. Toraldo di Francia, Nuovo Cimento **16**, 61 (1960).
[3]A. Yariv and C. C. Shih, Opt. Commun. **24**, 233 (1978).
[4]A. Gover and Z. Livni, Opt. Commun. **26**, 375 (1978).
[5]J. M. Wachtel, J. Appl. Phys. **50**, 49 (1979).
[6](a) R. L. Leavitt, D. E. Wortman, and H. Dropkin, IEEE J. Quantum Electron. **17**, 1333 (1981); (b) R. P. Leavitt, D. E. Wortman, and C. A. Morrison, Appl. Phys. Lett. **35**, 363 (1979).
[7]V. L. Bratman, G. G. Denisov, M. M. Ofitserov, S. D. Korovin, S. D. Polevin, and V. V. Rostov, IEEE Trans. Plasma Sci. **15**, 2 (1987).
[8]See also preliminary reports: L. Schächter and A. Ron, Appl. Phys. Lett. **53**, 828 (1988); J. Appl. Phys. (to be published).
[9]J. L. Uretsky, Ann. Phys. (N.Y.) **3**, 400 (1965).
[10](a) S. T. Peng, T. Tamir, and H. L. Bertoni, IEEE Trans. Microwave Theory Tech. **23**, 123 (1975); (b) P. C. Waterman, J. Acoust. Soc. Am. **57**, 791 (1975).
[11]*Electromagnetic Theory of Gratings,* edited by R. Petit (Springer-Verlag, Berlin, 1980).
[12]Lord Rayleigh (J. W. Strutt), Proc. R. Soc. London, Ser. A **79**, 399 (1907).
[13]B. A. Lippmann, J. Opt. Soc. Am. **43**, 408 (1953).
[14]J. Lam, J. Math. Phys. **8**, 1053 (1967).
[15]R. D. Hazeltine, M. N. Rosenbluth, and A. M. Sessler, J. Math. Phys. **12**, 502 (1971).
[16]J. A. DeSanto, J. Math. Phys. **12**, 1913 (1971).
[17]J. A. DeSanto, J. Math. Phys. **13**, 336 (1972).
[18]A. Gover, P. Dvorkis, and U. Elisha, J. Opt. Soc. Am. **1**, 723 (1984).
[19]P. M. van den Berg, J. Opt. Soc. Am. **63**, 689 (1973).
[20]P. M. van den Berg, J. Opt. Soc. Am. **63**, 1588 (1973).
[21]P. M. van den Berg and T. H. Tan, J. Opt. Soc. Am. **64**, 325 (1974).
[22]A. Gover and A. Yariv, Appl. Phys. **16**, (1978).
[23]N. M. Kroll, in *Novel Sources of Coherent Radiation,* Vol. 5 of *Physics of Quantum Electronics,* edited by S. F. Jacobs, M. Sargent, and M. O. Scully (Addison-Wesley, Reading, MA, 1978), p. 115.
[24]L. Schächter, J. Appl. Phys. **61**, 2718 (1987).
[25]M. Botton and A. Ron, IEEE Trans. Plasma Sci. **16**, 225 (1988).